

## ENVIRONMENTAL STUDIES

## Greenhouse gas emissions from African lakes are no longer a blind spot

Alberto V. Borges<sup>1\*</sup>, Loris Deirmendjian<sup>1†</sup>, Steven Bouillon<sup>2</sup>, William Okello<sup>3</sup>, Thibault Lambert<sup>1‡</sup>, Fleur A. E. Roland<sup>1</sup>, Vao F. Razanamahandry<sup>2</sup>, Ny Riavo G. Voarintsoa<sup>2§</sup>, François Darchambeau<sup>1¶</sup>, Ismael A. Kimirei<sup>4</sup>, Jean-Pierre Descy<sup>1</sup>, George H. Allen<sup>5</sup>, Cédric Morana<sup>1,2</sup>

Natural lakes are thought to be globally important sources of greenhouse gases (CO<sub>2</sub>, CH<sub>4</sub>, and N<sub>2</sub>O) to the atmosphere although nearly no data have been previously reported from Africa. We collected CO<sub>2</sub>, CH<sub>4</sub>, and N<sub>2</sub>O data in 24 African lakes that accounted for 49% of total lacustrine surface area of the African continent and covered a wide range of morphology and productivity. The surface water concentrations of dissolved CO<sub>2</sub> were much lower than values attributed in current literature to tropical lakes and lower than in boreal systems because of a higher productivity. In contrast, surface water–dissolved CH<sub>4</sub> concentrations were generally higher than in boreal systems. The lowest CO<sub>2</sub> and the highest CH<sub>4</sub> concentrations were observed in the more shallow and productive lakes. Emissions of CO<sub>2</sub> may likely have been substantially overestimated by a factor between 9 and 18 in African lakes and between 6 and 26 in pan-tropical lakes.

## INTRODUCTION

A better understanding of the aquatic biogeochemical cycle of greenhouse gases (GHGs; CO<sub>2</sub>, CH<sub>4</sub>, and N<sub>2</sub>O) and a more precise estimate of GHGs emissions at regional and global scales are essential to implement realistic pathways to attenuate climate change and assess the effectiveness of mitigation strategies. The emission of GHGs from inland waters (streams, rivers, lakes, and reservoirs) to the atmosphere could be important for global budgets (1–5), although estimates are very poorly constrained. For lakes, this is due to a general low data coverage of GHGs that is additionally geographically skewed, with an overrepresentation in global datasets of North America and Scandinavia, while tropical regions are much less covered. Tropical lakes (representing 13% of the global lake surface area) accounted for 34% of the global lake CO<sub>2</sub> emission, although they were represented by only 1.5% of the CO<sub>2</sub> dataset used in the global estimate of a zonally explicit scaling study of lacustrine CO<sub>2</sub> fluxes (4). Data used for tropical regions had been obtained mainly in South America but were virtually nonexistent in African systems, although they contributed to a third of the estimated tropical lacustrine CO<sub>2</sub> emissions.

This lack of data in tropical lakes is a major impediment for global extrapolations because cycling of GHGs in tropical lakes cannot be readily understood from the principles that apply to temperate and boreal systems. Annually integrated primary production is

potentially three times higher in tropical lakes (per unit of area) than in their temperate and boreal counterparts (based on theoretical considerations) (6). This is due to light and temperature conditions that are favorable for phytoplankton development year-round in tropical lakes but only during spring–summer in boreal and temperate lakes (6). In tropical lakes, a less vertically stable water column is favorable to nutrient inputs from deep to surface waters, but in temperate and boreal lakes, strong thermal vertical gradients in summer (when light conditions are most favorable) limit vertical nutrient inputs. Another notable difference is the higher content (by a factor of ~2) of dissolved organic carbon (DOC) in surface soils in boreal regions in North America and Scandinavia (where the bulk of lacustrine CO<sub>2</sub> data have been acquired so far) compared to tropical regions, even in rainforests (7). High DOC content in surface soils should enhance the hydrological transfer of DOC from soils to lakes and lead to an increase of the CO<sub>2</sub> content that usually correlates to DOC concentration in boreal lakes (2, 8). Conversely, enhanced heterotrophic activity due to higher year-round temperatures in tropical lakes has been assumed to support high aquatic CO<sub>2</sub> production and emission to the atmosphere (9, 10). The East African rift valley is the second major locus of large lakes on Earth after North America, yet it is nearly uncharted in terms of their GHGs emissions.

## RESULTS AND DISCUSSION

## Humic content and lake morphology explain the interlake variability of GHGs

Data on dissolved concentrations of CO<sub>2</sub>, CH<sub>4</sub>, and N<sub>2</sub>O were collected in surface waters of 24 natural lakes (Fig. 1 and tables S1 and S2), covering a wide range of altitude (9 to 2536 m), surface area (0.2 to 67,075 km<sup>2</sup>), average depth (0.1 to 572 m), surface water temperature (19.4° to 34.9°C), physical structure (holomictic to meromictic), and catchment land cover (savannah versus rainforest). This wide range of morphological and physiographical attributes was reflected in an equally wide range in medians of the partial pressure of CO<sub>2</sub> (pCO<sub>2</sub>) [11 to 3143 parts per million (ppm)], CH<sub>4</sub> concentration

Copyright © 2022  
The Authors, some  
rights reserved;  
exclusive licensee  
American Association  
for the Advancement  
of Science. No claim to  
original U.S. Government  
Works. Distributed  
under a Creative  
Commons Attribution  
NonCommercial  
License 4.0 (CC BY-NC).

<sup>1</sup>Chemical Oceanography Unit, University of Liège, Liège, Belgium. <sup>2</sup>Department of Earth and Environmental Sciences, KU Leuven, Leuven, Belgium. <sup>3</sup>Department of Limnology, National Fisheries Resource Research Institute, Jinja, Uganda. <sup>4</sup>Tanzania Fisheries Research Institute, Dar es Salaam, Tanzania. <sup>5</sup>Department of Geography, Texas A&M University, College Station, TX, USA.

\*Corresponding author. Email: alberto.borges@uliege.be

†Present address: Géosciences Environnement Toulouse UMR 5563 and UR 234 IRD, Université Paul-Sabatier, Toulouse, France.

‡Present address: Institute of Earth Surface Dynamics, University of Lausanne, Lausanne, Switzerland.

§Present address: Department of Earth and Atmospheric Science, University of Houston, Texas, USA.

¶Present address: Direction générale opérationnelle Agriculture, Ressources Naturelles et Environnement, Service Public de Wallonie, Namur, Belgium.

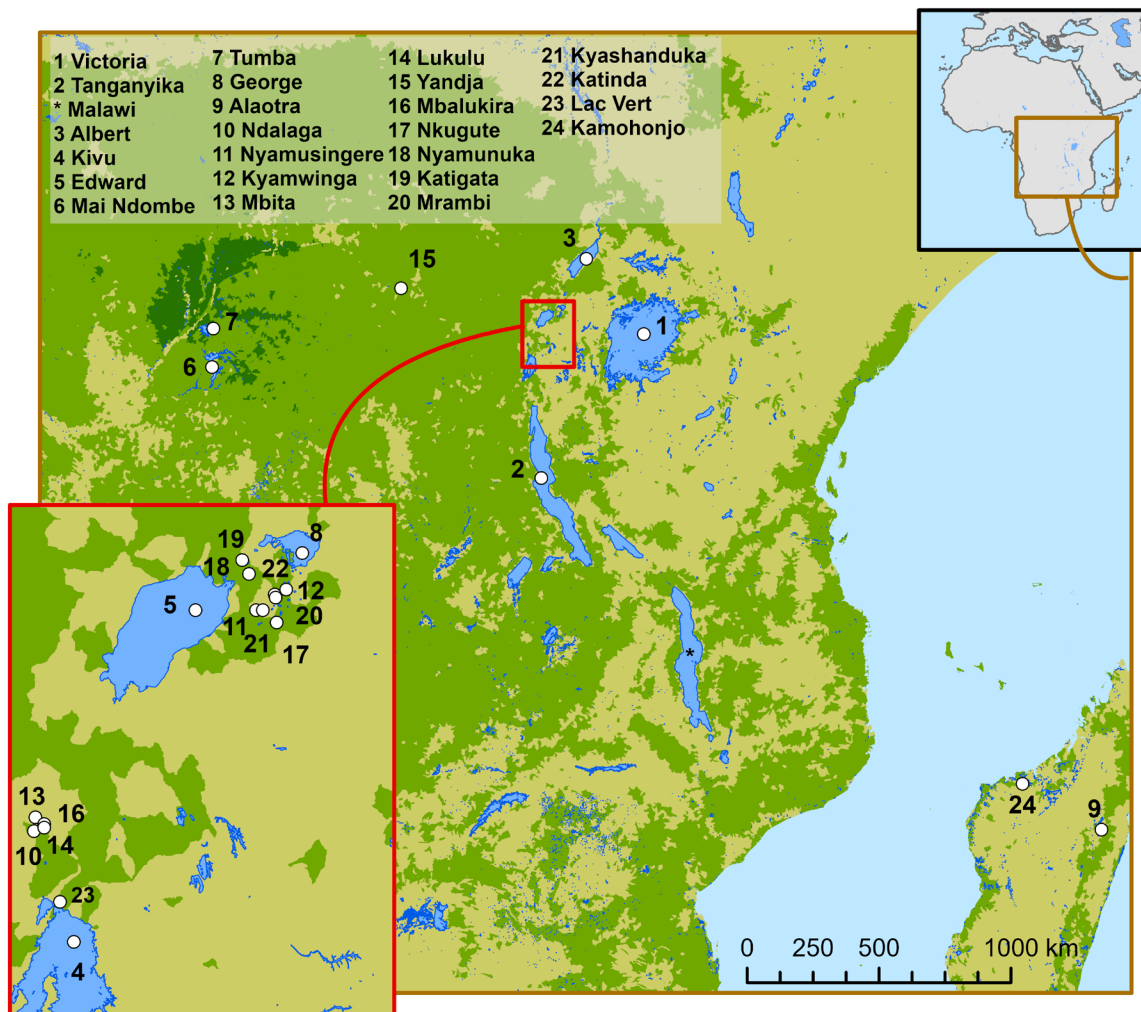


**Fig. 1. Location of the 24 sampled African lakes, plus Lake Malawi (48).** This dataset of CO<sub>2</sub>, CH<sub>4</sub>, and N<sub>2</sub>O in surface waters covers a wide range of morphological conditions (surface area and depth), water column physical structure, catchment land cover, and lake productivity. Map indicates cover by savannah, forest, and flooded forest (from lightest to darkest shade of green).

(19 to 490,749 nM), N<sub>2</sub>O saturation level (%N<sub>2</sub>O) (8 to 381%), and phytoplankton biomass as indicated by the chlorophyll a (Chl-a) concentration (0.5 to 1,170 μg liter<sup>-1</sup>).

We distinguished nonhumic lakes from humic lakes that are characterized by high concentrations of DOC and colored dissolved organic matter (CDOM) of terrigenous origin, characterized by low values of slope ratio (SR) (11). Consequently, we used the SR of CDOM (11) as a separation criterion and classified lakes with an SR < 1 as humic and lakes with an SR > 1 as nonhumic. In temperate and boreal lakes, these two types of lakes differ in terms of phytoplankton productivity and overall carbon cycling (12), and we hypothesize that they also behave differently in terms of the dynamics of GHGs (13).

The four sampled humic lakes (Mai Ndombe, Tumba, Alaotra, and Kamohonjo) showed higher pCO<sub>2</sub> and %N<sub>2</sub>O and lower Chl-a values than the other (nonhumic) lakes at similar average depths and surface areas (Fig. 2). The pCO<sub>2</sub> and %N<sub>2</sub>O values were negatively related to CDOM SR (Fig. 3 and fig. S1), showing that the content of these two GHGs increased with humic content of the sampled lakes. Dissolved CH<sub>4</sub> concentrations were unrelated to CDOM SR.

The average pCO<sub>2</sub> and %N<sub>2</sub>O values in nonhumic lakes were positively related to both lake surface area and average depth, while CH<sub>4</sub> and Chl-a were negatively related to these morphological variables (Fig. 2). Surface waters were always oversaturated in CH<sub>4</sub> relative to the atmosphere. Among nonhumic lakes, smaller (shallower) lakes were generally undersaturated in CO<sub>2</sub> and N<sub>2</sub>O relative to the atmosphere (i.e., acting as atmospheric sinks for both these gases), while larger (deeper) lakes were close to equilibrium with the atmosphere (slightly above or below saturation). Humic lakes, in contrast, were markedly oversaturated in CO<sub>2</sub> and N<sub>2</sub>O (Fig. 2).

At the scale of individual lakes, CH<sub>4</sub> also followed a decreasing pattern as a function of depth (Fig. 4). At shallow depths (<10 m), the highest CH<sub>4</sub> values were observed in Lakes Victoria and Albert compared to Lakes Tanganyika and Edward. At depths >40 m, the CH<sub>4</sub> in surface waters of Lake Tanganyika was higher than Lakes Victoria and Albert (Fig. 4). This pattern was consistent with the meromictic nature of Lake Tanganyika that leads to very high concentrations of CH<sub>4</sub> in bottom anoxic waters, higher than in the holomictic Lakes Edward and Victoria (fig. S2), where CH<sub>4</sub> content in

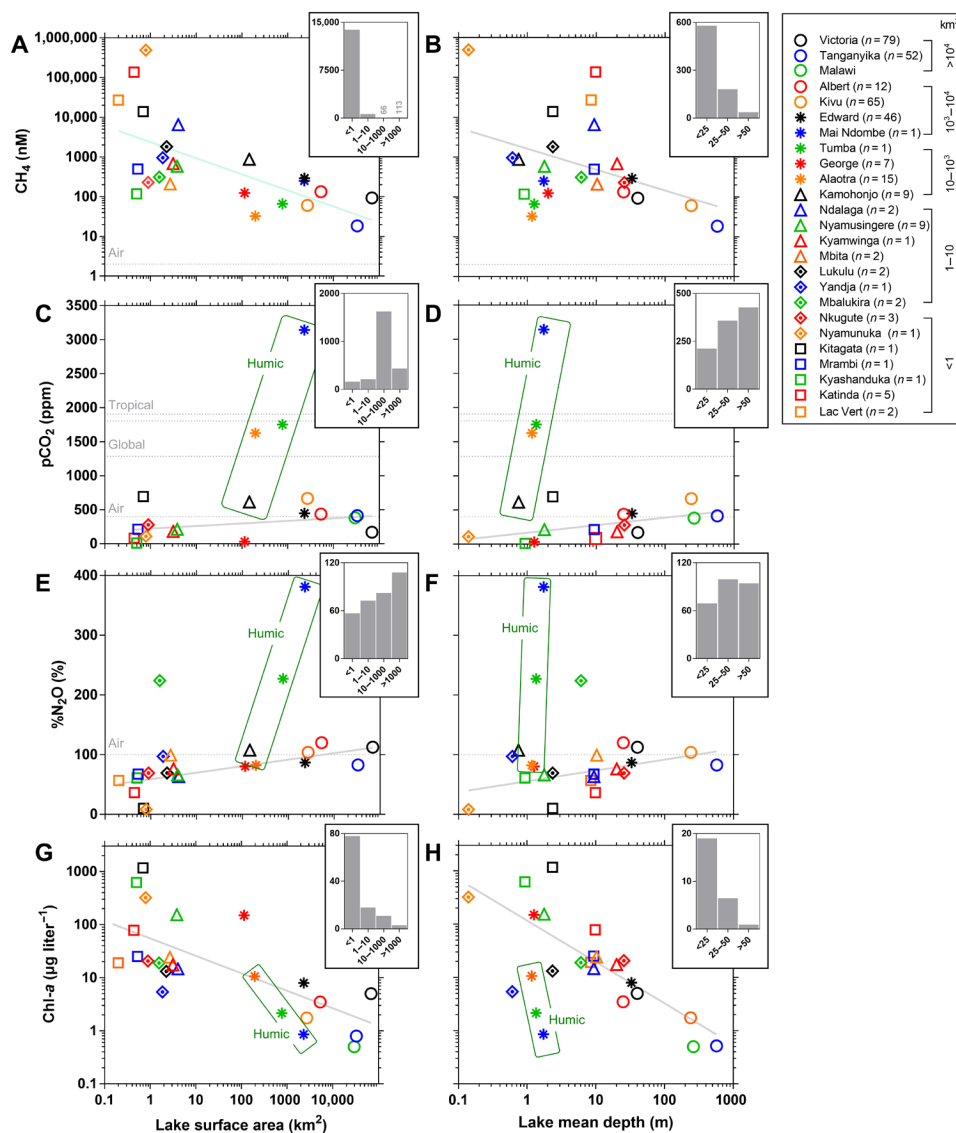


**Fig. 2. Lake morphology controls  $\text{CH}_4$ ,  $\text{N}_2\text{O}$ , and  $\text{CO}_2$  in lacustrine surface waters.** Surface water–dissolved  $\text{CH}_4$  concentration (A and B),  $\text{pCO}_2$  (C and D),  $\text{N}_2\text{O}$  saturation level ( $\%\text{N}_2\text{O}$ ) (E and F), and Chl-a concentration (G and H) in 24 African tropical lakes versus lake surface area and average depth. For lakes where multiple measurements were made, the symbol shows the median ( $n$  indicates the number of samplings, detailed in table S7). Insets show data binned (median) by classes of surface area or depth. Horizontal dotted lines indicate the atmospheric equilibrium of the three gases, additionally for  $\text{CO}_2$  two average estimates for tropical (4, 7) and global lakes (1). Solid lines are fits to the data (table S3) from which humic lakes were excluded for  $\text{pCO}_2$  and  $\%\text{N}_2\text{O}$ . Data of  $\text{pCO}_2$  in Lake Malawi were obtained by another group but with a comparable high-quality method (equilibrator coupled to an infrared  $\text{CO}_2$  analyzer) (48).  $\text{CO}_2$  and  $\%\text{N}_2\text{O}$  data in humic lakes were clustered but did not show a pattern with lake surface and mean depth, so the median was used to upscale the values at continental scale.  $\text{CO}_2$  and  $\%\text{N}_2\text{O}$  in nonhumic lakes were positively related to mean depth and these relations were used to scale the values at continental scale.  $\text{CH}_4$  was negatively related to mean depth, irrespective of the lake type, and this relation was used to scale values at continental scale.

bottom waters strongly varies seasonally with changes in vertical thermal stratification and oxygenation levels (fig. S3).

### A complex combination of sources and sinks of GHGs

The content of  $\text{CO}_2$ ,  $\text{CH}_4$ , and  $\text{N}_2\text{O}$  in surface waters of lakes results from the balance of several sources and sinks that are specific to each gas (listed and explained in figs. S4 to S6). The relative importance of these sources and sinks varies as a function of external drivers (e.g., inputs of allochthonous organic matter and nutrients) and internal drivers (e.g., organic matter production and degradation),

related to catchment properties (land cover), lake morphology (size and shape), and climate (precipitation). Lake surface area and depth are simple metrics and have been shown to be good predictors in boreal lakes of  $\text{CO}_2$  and  $\text{CH}_4$  concentrations [e.g., (14)], as well as of aquatic ecosystem metabolism (15) defined as the balance between production of autochthonous organic (primary production,  $P$ ) and degradation of organic matter (respiration,  $R$ ).

In nonhumic lakes,  $\text{pCO}_2$  values were lower in the smallest and shallower lakes (Fig. 2). We interpret this pattern as resulting from higher phytoplankton biomass and  $P$  in shallower lakes, as shown

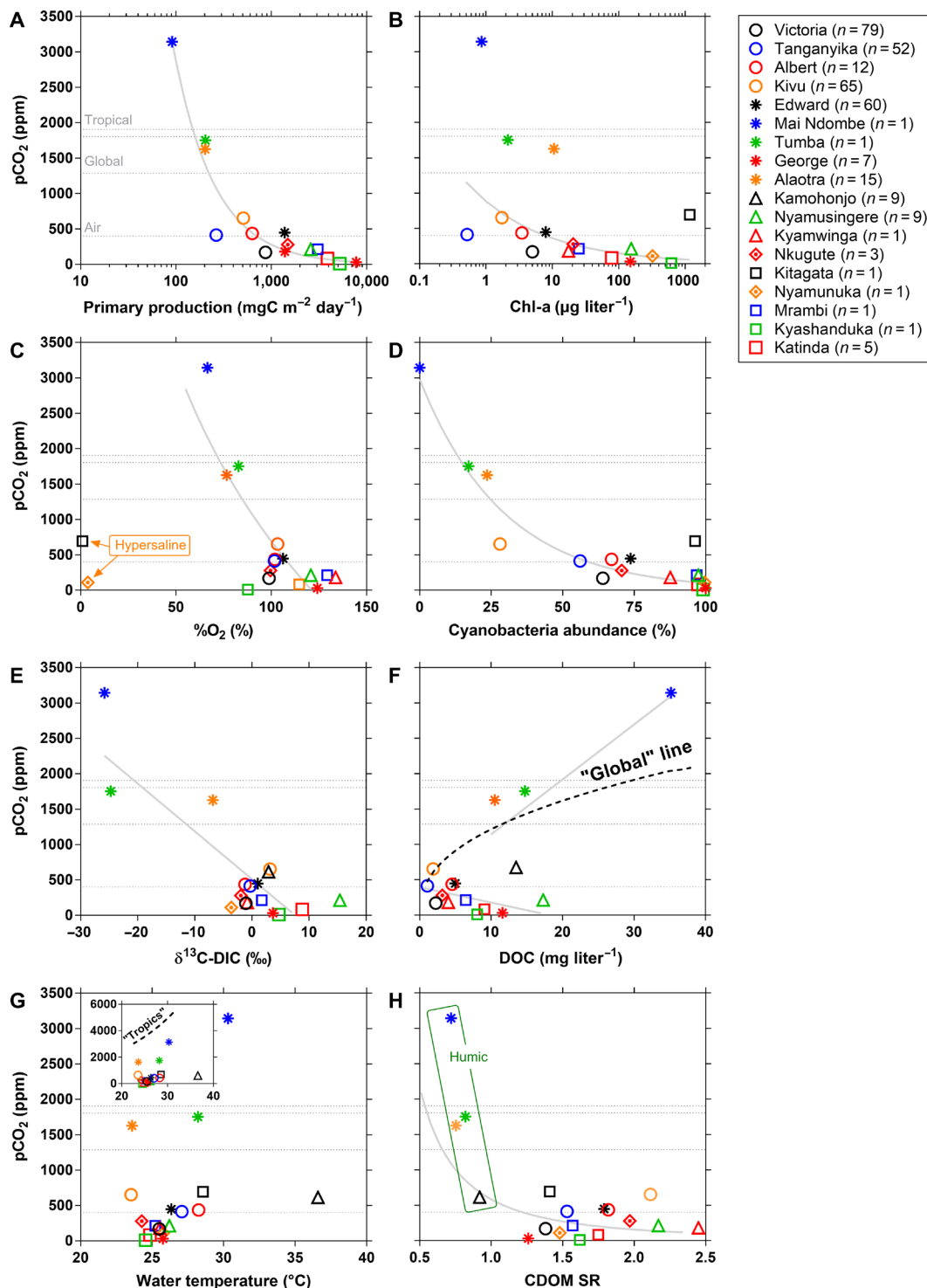


**Fig. 3. CO<sub>2</sub> levels are highly variable among African lakes and patterns depend on primary production.** Surface water pCO<sub>2</sub> in several African tropical lakes versus pelagic aquatic primary production (A), Chl-a concentration (B), oxygen saturation level (%O<sub>2</sub>) (C), cyanobacteria abundance (D), carbon stable isotope composition of dissolved inorganic carbon ( $\delta^{13}\text{C-DIC}$ ) (E), DOC (F), water temperature (G), and CDOM SR (H). Dotted lines and solid lines as in Fig. 2. The black dotted line in the inset gives the relation of pCO<sub>2</sub> versus DOC from a global dataset (2), while the black dotted line in the inset gives the relation of pCO<sub>2</sub> versus temperature from a dataset of tropical lakes (9). For lakes where multiple measurements were made, the symbol shows the median ( $n$  indicates the number of pCO<sub>2</sub> measurements).

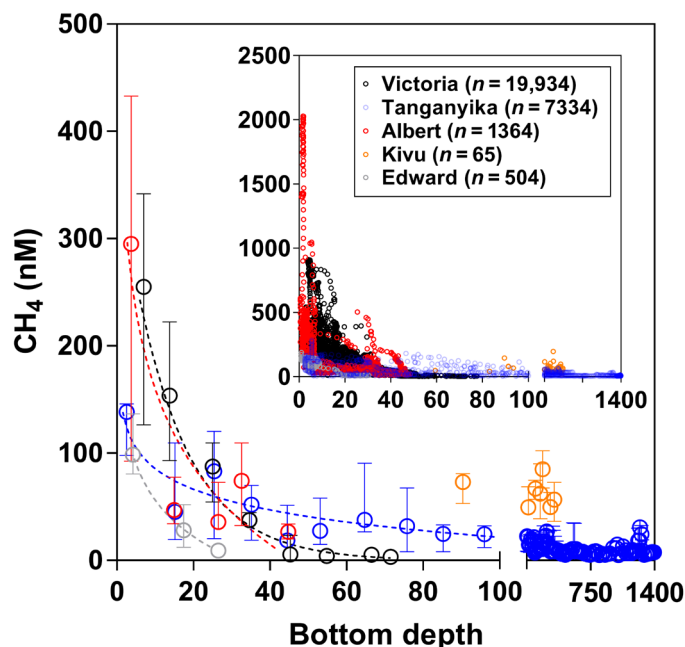


**Fig. 4. CH<sub>4</sub> strongly varies as a function of bottom depth within lakes.** Continuous measurements of dissolved CH<sub>4</sub> concentrations were made in Lakes Victoria, Tanganyika, Albert, Kivu, and Edward, with an equilibrator connected to a laser spectrometer except for Lake Kivu (compilation of 65 discrete samples measured by headspace with a gas chromatograph obtained during five cruises; *n* indicates the number of measurements). The inset shows the raw data, and the main panel shows the data binned by depth intervals of 10. Dotted lines are the curves fitted to data (table S3). Data bins per depth interval were combined with bathymetry maps to derive CH<sub>4</sub> (and pCO<sub>2</sub>; not shown here) values spatially representative of the largest lakes, accounting for the strong horizontal gradients as a function of depth.

by the negative relation between Chl-*a* and depth (Fig. 2). This is probably due to the proximity of surface waters and the sediment in shallow lakes that allows a replenishment of surface waters in nutrients diffusing from the sediment (15). Nonhumic large lakes were characterized by lower phytoplankton biomass (Fig. 2) due to increasing depth and disconnection between surface (illuminated) waters and the nutrient-rich deeper waters. In parallel, the relative importance of terrestrial (allochthonous) organic and inorganic carbon inputs decreases relative to lake area and volume, hence having a lower impact on CO<sub>2</sub> levels in larger lakes (fig. S4). In larger lakes, higher gas transfer velocity (*k*) values (16) contribute to the equilibration of surface waters (this applies to the three gases). The combination of these putative drivers (see also fig. S4) could explain the general positive relationship between pCO<sub>2</sub> and lake size (surface area and depth) that we observed in nonhumic lakes (Fig. 2).

In humic lakes, high CDOM content decreases light penetration in the water column, strongly limiting phytoplankton growth and planktonic *P*, and the high content of terrestrial DOC should also sustain microbial degradation of organic matter (12). In addition, the sampled humic lakes were characterized by important wetland coverage (table S1) that should have sustained a large lateral input to the lakes of CO<sub>2</sub> from flooded soils (17). The combination of these putative drivers could explain the higher pCO<sub>2</sub> values observed in the humic lakes than in nonhumic lakes at similar depths or surface areas (Fig. 2); this interpretation agrees with the general patterns of pCO<sub>2</sub> and other variables shown in Fig. 3.

When combining data from both humic and nonhumic lakes, pCO<sub>2</sub> was negatively related to *P* and Chl-*a* (Fig. 3). In shallow lakes, extremely high Chl-*a* values were attained (Fig. 2) related to the occurrence of cyanobacteria. Numerous species of cyanobacteria can overcome nitrogen (N) limitation through N<sub>2</sub>-fixation, as well as CO<sub>2</sub> limitation (by using HCO<sub>3</sub><sup>-</sup> for photosynthesis) and light limitation because of higher light harvesting capabilities than most other phytoplankton groups (18). Together, these features provide cyanobacteria with a competitive advantage in warm, productive, and shallow waters over other phytoplankton groups (18). This could then possibly explain the general negative relationship between pCO<sub>2</sub> and the abundance of cyanobacteria observed in the sampled lakes (Fig. 3). Relations between pCO<sub>2</sub> and other variables can also be interpreted as resulting from a dominance of organic matter degradation in humic lakes and a stronger influence of carbon fixation by phytoplankton in nonhumic lakes. The negative relationship between pCO<sub>2</sub> and the carbon stable isotope composition of dissolved inorganic carbon (δ<sup>13</sup>C-DIC) possibly resulted from a combination of two processes: (i) the input of CO<sub>2</sub> in humic lakes from the degradation of plant organic matter with mostly a C<sub>3</sub> photosynthetic pathway (woody plants and trees have δ<sup>13</sup>C values of ~-27‰), leading to low δ<sup>13</sup>C-DIC values and high pCO<sub>2</sub> values and (ii) the preferential removal of dissolved <sup>12</sup>CO<sub>2</sub> by emission to the atmosphere and of the uptake of <sup>12</sup>CO<sub>2</sub> by photosynthesis in nonhumic lakes leading to higher δ<sup>13</sup>C-DIC values and low pCO<sub>2</sub> values. Note that there were no clear patterns between CO<sub>2</sub> levels and HCO<sub>3</sub><sup>-</sup> levels in the sampled African lakes (fig. S7). %O<sub>2</sub> levels can also be used as indicators of ecosystem metabolism, and in general, the lakes with low pCO<sub>2</sub> were also oversaturated in O<sub>2</sub>, except in two hypersaline lakes (Kitagata and Nyamunuka) where %O<sub>2</sub> values were very low and deviated from the general pCO<sub>2</sub>-%O<sub>2</sub> pattern, likely because of chemical consumption of O<sub>2</sub> from the oxidation of H<sub>2</sub>S diffusing from the sediments to surface waters. Both the air-water gradient of pCO<sub>2</sub> (ΔpCO<sub>2</sub>) and air-water CO<sub>2</sub> flux (FCO<sub>2</sub>) showed an increasing sink of atmospheric CO<sub>2</sub> with lake net autotrophy, quantified by the ratio of planktonic *P* to *R* above 1 and a positive net ecosystem production (NEP = *P* - *R*) (Fig. 5). The lack of relation between pCO<sub>2</sub> in the sampled lakes and terrestrial vegetation biomass on the catchment (fig. S8) suggests two possible explanations: (i) The effects of the variations of lake size (Fig. 2 and fig. S4) have a stronger influence on CO<sub>2</sub> dynamics than the variations of the inputs of allochthonous carbon due to changes in terrestrial vegetation biomass, and/or (ii) internal processes independent of allochthonous carbon inputs also control CO<sub>2</sub> levels in these lakes, particularly planktonic *P* in nonhumic shallow lakes.

There were no clear differences between humic and nonhumic lakes in CH<sub>4</sub> as a function of lake surface area and mean lake depth (Fig. 2). The highest CH<sub>4</sub> concentrations were observed in the shallowest lakes (Fig. 2). This might reflect the relatively higher input of CH<sub>4</sub> from sediments to the water per unit of water volume in the shallowest lakes (fig. S5). Conversely, in the deeper and larger lakes, deeper mixed layers might promote microbial methane oxidation (MOX), while more marked thermal vertical stratification isolates the epilimnion (where CH<sub>4</sub> is removed by MOX and by the emission to the atmosphere) from the hypolimnion (where CH<sub>4</sub> accumulates) (fig. S5). In addition, shallower lakes were also the most productive (Fig. 2); hence, there should have been a larger delivery to the sediments of fresh organic matter from phytoplankton detritus. This, in turn, should lead to intense benthic organic matter

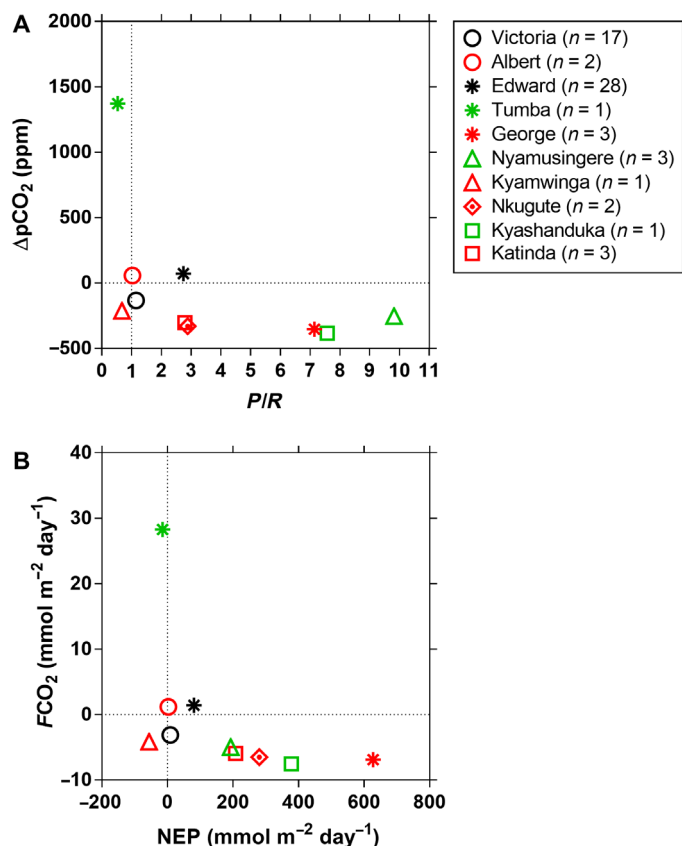


**Fig. 5. Net ecosystem autotrophy drives a CO<sub>2</sub> sink in most of the studied African lakes.** Variations in several African tropical lakes of the air-water gradient of the pCO<sub>2</sub> ( $\Delta p\text{CO}_2$ ) as a function of the ratio of aquatic pelagic primary production ( $P$ ) and community respiration ( $R$ ) (A) and the air-water CO<sub>2</sub> flux ( $F\text{CO}_2$ ) as a function of NEP (B).  $P/R > 1$  and  $\text{NEP} > 0$  correspond to net autotrophy at the community level and is, in most cases, associated with being a sink of atmospheric CO<sub>2</sub> ( $\Delta p\text{CO}_2 < 0$ ,  $F\text{CO}_2 < 0$ ). For lakes where multiple measurements were made, the symbol shows the median ( $n$  indicates the number of measurements).

degradation including methanogenesis and, consequently, high sediment-water CH<sub>4</sub> fluxes (fig. S9). The combination of these putative drivers (fig. S5) could explain the general negative relation between CH<sub>4</sub> and lake depth and surface area that we report across different lakes (Fig. 2), as well as the variations with bathymetry within a single lake (Fig. 4). Furthermore, this might also explain the positive correlation between CH<sub>4</sub> and Chl-a (Fig. 6). Such a relation has been previously interpreted by some studies as resulting from the production of CH<sub>4</sub> in aerobic conditions (19), either directly (20) or indirectly (21) linked to phytoplankton metabolism. Although production of CH<sub>4</sub> in aerobic conditions linked to phytoplankton metabolism was shown to occur in five African lakes, the related input flux to the water column was orders of magnitude lower than sedimentary CH<sub>4</sub> inputs to the water column (22). In nonhumic lakes, high phytoplankton biomass also led to low CO<sub>2</sub> values that, combined with high CH<sub>4</sub>, also resulted in an overall positive relation between the CH<sub>4</sub>:CO<sub>2</sub> ratio and Chl-a (Fig. 6).

In nonhumic lakes, %N<sub>2</sub>O was negatively related to lake depth (Fig. 2), being close to atmospheric equilibrium in the deeper lakes and below atmospheric equilibrium in the shallowest lakes. In these lakes with low dissolved inorganic N (DIN) levels, sedimentary

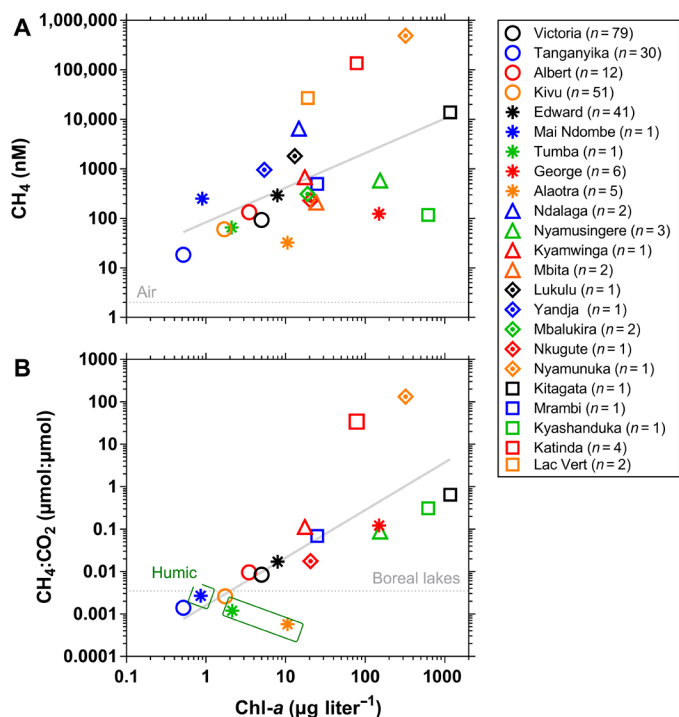


**Fig. 6. CH<sub>4</sub> levels in surface waters of African lakes are driven by lacustrine productivity.** Dissolved CH<sub>4</sub> concentrations (A) and ratio of dissolved CH<sub>4</sub> and CO<sub>2</sub> concentrations (B) versus Chl-a concentration in surface waters of several African tropical lakes. Horizontal dotted line represents the equilibrium with the atmosphere (top) and the average value for boreal lakes (26). Solid line is a fit to the data (table S3). For lakes where multiple measurements were made, the symbol shows the median ( $n$  indicates the number of measurements). For CH<sub>4</sub>, no relation was observed with other measured variables. The positive relation of CH<sub>4</sub> and Chl-a should be interpreted as resulting from the dependence of CH<sub>4</sub> in surface waters from sedimentary CH<sub>4</sub> fluxes to the water column (22) that were higher in shallow and productive systems (fig. S9), while in stratified deep systems, the CH<sub>4</sub> removal by MOX led to low-surface CH<sub>4</sub> (49).

denitrification could be involved in the uptake of N<sub>2</sub>O from the water-column and explain the observed N<sub>2</sub>O undersaturation (figs. S6 and S9). The N<sub>2</sub>O undersaturation was more marked in the shallowest nonhumic lakes where intense sedimentary denitrification rates, sustained by high organic matter deposition on the sediments (phytoplankton detritus), should occur.

In humic lakes, N<sub>2</sub>O was distinctly above atmospheric equilibrium (Fig. 2), indicating sedimentary or water column N<sub>2</sub>O net production. In humic lakes, low phytoplankton  $P$  and microbial mineralization of organic matter led to relatively higher levels of DIN (23) that can sustain N<sub>2</sub>O production (fig. S6). The combination of these putative drivers could explain the negative relations between %N<sub>2</sub>O and primary production, Chl-a, and CDOM SR and the positive relation between %N<sub>2</sub>O and DOC concentrations (fig. S1).

### Comparison with boreal and other tropical lakes of GHGs

The increase of CH<sub>4</sub> and the decrease of CO<sub>2</sub> with phytoplankton biomass (Figs. 3 and 6) led to higher CH<sub>4</sub> and lower CO<sub>2</sub> values in surface waters in African lakes compared to boreal systems (Fig. 7) where phytoplankton biomass is typically low and seasonally restricted to spring and summer. Higher temperatures in tropical lakes compared to boreal lakes are also more favorable for methanogenesis

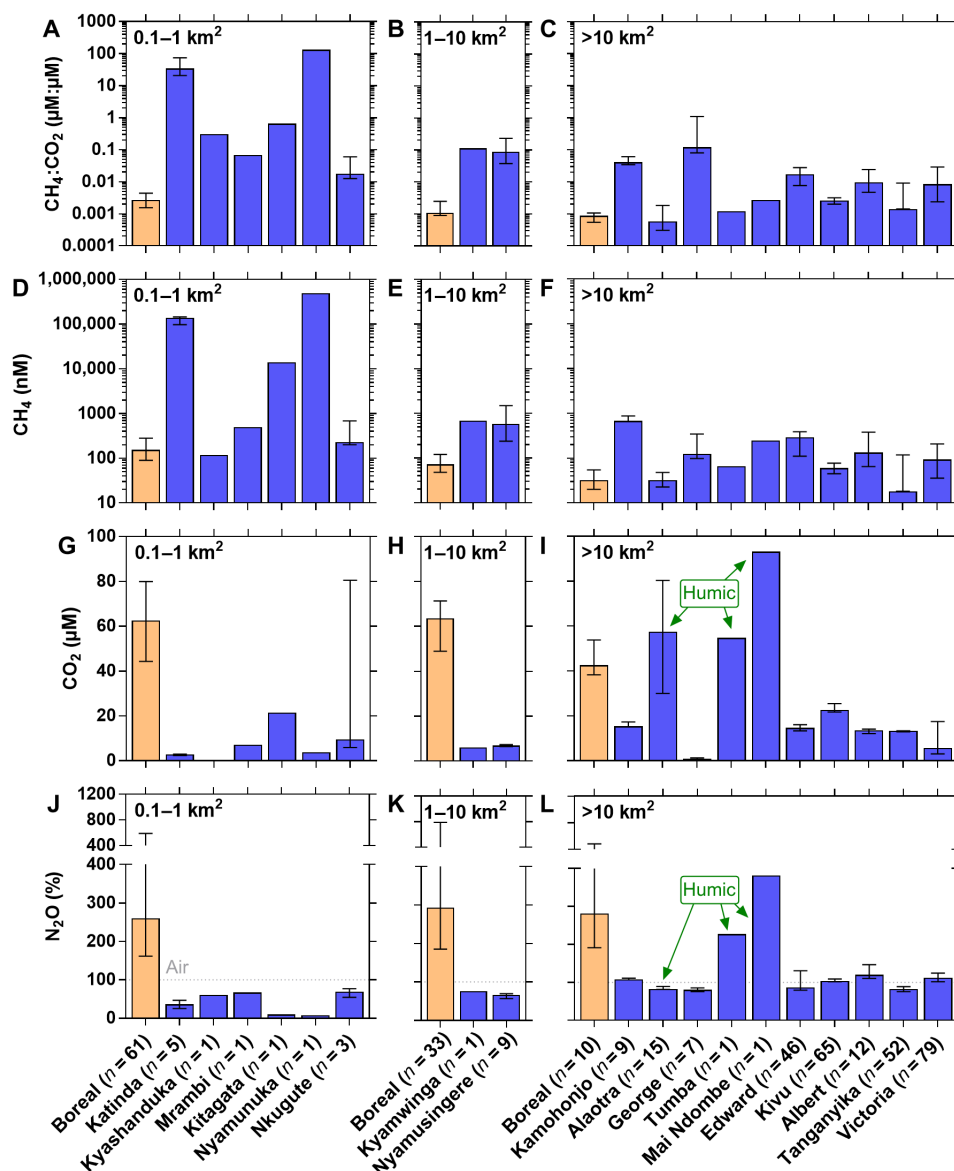


**Fig. 7. CH<sub>4</sub> is higher and CO<sub>2</sub> is lower in African lakes than in boreal lakes.** The ratio of dissolved CH<sub>4</sub> and CO<sub>2</sub> concentrations (A to C), dissolved CH<sub>4</sub> (D to F), CO<sub>2</sub> (G to I) concentrations, and N<sub>2</sub>O saturation levels (%N<sub>2</sub>O) (J to L) in surface waters of several African tropical lakes compared to paired CO<sub>2</sub> and CH<sub>4</sub> measurements ( $n = 224$ ) in lakes located in the boreal climatic zone compiled from literature in (26) located in Finland, Canada, Siberia (latitude, >60°N) and %N<sub>2</sub>O in Finland (50) sorted into three size classes (0.1 to 1 km<sup>2</sup>, 1 to 10 km<sup>2</sup>, and >10 km<sup>2</sup>). Surface water temperature in boreal lakes was 9.8°C (median) versus 25.8°C in African lakes. Box indicates the median; bars indicate the first and third quartile.  $n$  indicates the number of data points.

(24). Comparatively higher soil DOC content at boreal latitudes (7) should also lead to a stronger enrichment in terrestrial DOC in boreal lakes compared to tropical lakes of similar size. As CO<sub>2</sub> increases with DOC in boreal lakes (8, 13), this could also help explain why the CO<sub>2</sub> values in boreal lakes were higher than in African lakes (Fig. 7). Only in three African humic lakes was CO<sub>2</sub> higher than the median in large boreal lakes (Fig. 7). Boreal lakes were strongly oversaturated in %N<sub>2</sub>O compared to tropical African lakes that were undersaturated for the smaller ones (surface area, <10 km<sup>2</sup>), while larger ones (surface area, >10 km<sup>2</sup>) were close to saturation, except for two humic ones in which %N<sub>2</sub>O values were comparable to values in boreal lakes (Fig. 7).

The pCO<sub>2</sub> values in 22 lakes were lower than the values reported in the literature as representative for lakes globally (1) and the tropics (4, 9) except for three of the humic lakes (Fig. 2). In addition, pCO<sub>2</sub> values in the sampled African lakes were below the relationship of pCO<sub>2</sub> as a function of temperature assumed to be representative of the tropics (Fig. 3G) (9), and most of our pCO<sub>2</sub> values were below the relationship for pCO<sub>2</sub> versus DOC for lakes globally (Fig. 3F) (2). In nonhumic lakes, pCO<sub>2</sub> was negatively related to DOC (Fig. 3F) most likely originating from phytoplankton exudates, as confirmed by the high CDOM SR values (Fig. 3H) and by the positive relation between DOC and Chl-*a* and cyanobacteria relative abundance (Fig. 8). In humic lakes, however, pCO<sub>2</sub> was positively related to

DOC as previously reported (2, 8). Consequently, a positive correlation between pCO<sub>2</sub> and DOC does not seem to be a universal feature as frequently reported in literature (2, 8), and in African lakes, it only applied to humic lakes. Note also that we report a positive relation between pCO<sub>2</sub> and lake surface area in nonhumic lakes (Fig. 2), although a negative relation between these variables has been repeatedly reported in boreal lakes at the local (25), regional (8, 14), and global scale (4, 26).

The surface area-weighted average pCO<sub>2</sub> for the sampled African lakes (plus Lake Malawi) of 400 ppm was only slightly above atmospheric equilibrium (388 ppm) and distinctly lower than the reported average pCO<sub>2</sub> values in South American tropical lakes (1804 to 2270 ppm) (9, 10), which represent the bulk of data reported so far for tropical lakes. There could be several explanations for these differences, such as an overrepresentation of floodplain lakes and very small water bodies in the South American CO<sub>2</sub> datasets. The latter explanation is also consistent with a lower average pCO<sub>2</sub> value (1007 ppm) reported in 12 large (>500 km<sup>2</sup>) tropical lakes (27). In addition, most of these studies were based on data that were indirectly calculated from pH and total alkalinity (TA), when it has been shown that this method is prone to extremely large errors due to measurement biases on both pH and TA and tends to strongly overestimate CO<sub>2</sub> levels particularly in humic lakes characteristic of floodplains (28).

### GHG fluxes in African tropical and pan-tropical lakes

The FCO<sub>2</sub> and the air-water diffusive fluxes of CH<sub>4</sub> (FCH<sub>4</sub>) and N<sub>2</sub>O (FN<sub>2</sub>O) were upscaled for tropical lakes (24°S to 24°N) with a surface area >0.1 km<sup>2</sup>, at African and pan-tropical scales (Table 1). FCO<sub>2</sub>, FN<sub>2</sub>O, and diffusive FCH<sub>4</sub> per square meter were lower in nonhumic than humic lakes at African and pan-tropical scales (table S4). Lake Chad alone accounted for 47% of FCO<sub>2</sub>, 87% of diffusive FCH<sub>4</sub>, and 52% of FN<sub>2</sub>O integrated for African humic lakes (table S4). For the initial upscaling, we used the surface area for Lake Chad of 18,752 km<sup>2</sup> given by HydroLAKES (29), although recent remote sensing data provide a much lower value of 2603 km<sup>2</sup> for the 1989–2017 period (30), reflecting its marked shrinkage since the 1980s due to climate change, as this lake is very shallow and located in an arid climatic zone. FCO<sub>2</sub>, FCH<sub>4</sub>, and FN<sub>2</sub>O were re-computed using the more recent and more realistic surface area of Lake Chad (30), which we will consider hereafter as our nominal GHG flux values (Table 1).

The integrated FN<sub>2</sub>O for pan-tropical lakes was 16 times lower than estimated from a global model (31). In African tropical lakes, the integrated FN<sub>2</sub>O was negative, indicating a very small sink for atmospheric N<sub>2</sub>O, while the global model (31) predicted a small source of N<sub>2</sub>O to the atmosphere (Table 1). This global model computes N<sub>2</sub>O (and FN<sub>2</sub>O) from catchment N inputs and water

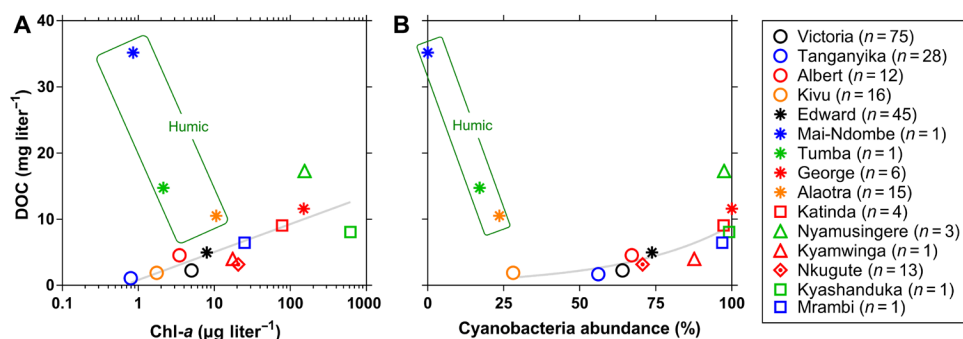


**Fig. 8. Allochthonous versus autochthonous origin of DOC in African lakes depends on type (humic versus nonhumic).** DOC versus Chl-a (A) concentration and versus cyanobacteria abundance (B) in surface waters of several African tropical lakes. Solid line is a fit to the data (table S3). For lakes where multiple measurements were made, the symbol shows the median (*n* indicates the number of measurements).

**Table 1. Downward reevaluation of tropical lacustrine CO<sub>2</sub>, CH<sub>4</sub>, and N<sub>2</sub>O emissions.** Air-water flux of CO<sub>2</sub> (FCO<sub>2</sub>), CH<sub>4</sub> (FCH<sub>4</sub>, diffusive and ebullitive), and N<sub>2</sub>O (FN<sub>2</sub>O) integrated for African tropical and pan-tropical lakes (with a surface area >0.1 km<sup>2</sup>) compared to previous estimates (details in table S4) (1, 3, 4, 9, 31, 47). Values with a single asterisk (\*) correspond to the scaling using the original HydroLAKES surface area (29), including an unrealistic surface area value of 18,752 km<sup>2</sup> for Lake Chad. Values with a double asterisk (\*\*) were obtained with a more recent surface area value of 2603 km<sup>2</sup> for Lake Chad (30). n.a., not available.

	FCO <sub>2</sub>	Diffusive FCH <sub>4</sub>	Ebullitive FCH <sub>4</sub>	FN <sub>2</sub> O
	TgC year <sup>-1</sup>	TgCH <sub>4</sub> year <sup>-1</sup>	TgCH <sub>4</sub> year <sup>-1</sup>	GgN <sub>2</sub> O-N year <sup>-1</sup>
<b>African tropical lakes</b>				
This study (*)	6.3 ± 1.9	1.3 ± 0.3	2.3 (0.8–5.5)	0.3 ± 0.2
This study (**)	3.3 ± 1.0	0.4 ± 0.1	1.8 (0.6–4.1)	–0.1 ± 0.1
Previous studies	35.6	n.a.	n.a.	3.7
<b>Pan-tropical lakes</b>				
This study (*)	20.5 ± 10.7	1.6 ± 0.4	4.9 (1.7–11.4)	0.8 ± 1.1
This study (**)	17.5 ± 9.5	0.7 ± 0.2	4.4 (1.5–10.0)	0.4 ± 0.7
Previous studies	103.1 to 441.6	3.1	22.2	6.5



residence time and accounts, also as a function of residence time, for the decrease of  $\text{N}_2\text{O}$  due to the reduction of  $\text{N}_2\text{O}$  to  $\text{N}_2$ , down to saturation but not below. The model cannot mathematically predict the undersaturation of  $\text{N}_2\text{O}$  that we observed in productive shallow lakes (Fig. 2) because it does not explicitly represent the denitrification process.

The integrated pan-tropical diffusive  $\text{CH}_4$  emission was 4.5 lower than the one previously reported (3), and the difference was mostly related to the differences in total lake surface area values, as the diffusive  $F\text{CH}_4$  per square meter was closer but still 2.5 times lower (table S4). We occasionally quantified ebullitive  $\text{CH}_4$  emissions, found to be  $\sim 20$  times higher than diffusive  $\text{CH}_4$  emissions in two shallow productive lakes (George and Nyamusingire), but ebullitive and diffusive  $\text{CH}_4$  fluxes were equivalent in deeper lakes (Edward and Victoria) (table S5). Combined with data reported mainly in South America (fig. S10), we estimated ebullitive  $\text{CH}_4$  emissions of 1.8 [interquartile range (IQR): 0.6 to 4.1]  $\text{TgCH}_4 \text{ year}^{-1}$  for African lakes and 4.4 (IQR: 1.5 to 10.0)  $\text{TgCH}_4 \text{ year}^{-1}$  for pan-tropical lakes (Table 1 and table S6). The pan-tropical  $\text{CH}_4$  ebullition emissions were six times lower than previously reported (3) because we only integrated the fluxes in the littoral zone (depth,  $<10$  m) with a surface area totaling 135,206  $\text{km}^2$ , while Bastviken *et al.* (3) integrated the fluxes over the total lacustrine area (585,536  $\text{km}^2$ ). The median ebullitive  $\text{CH}_4$  flux per square meter that we upscaled [4.4 (IQR: 1.5 to 10.7)  $\text{mmol m}^{-2} \text{ year}^{-1}$ ] was close to the one used in (3) ( $6.5 \pm 3.7$   $\text{mmol m}^{-2} \text{ year}^{-1}$ ). Yet, our  $\text{CH}_4$  ebullition flux could be underestimated since it is based on open water lake values, while vegetated habitats have been shown to have very high emission rates (32). The pan-tropical lacustrine  $\text{CH}_4$  emissions were dominated by ebullition compared to diffusion. The ratio of ebullitive to diffusive  $\text{CH}_4$  lacustrine flux was  $\sim 6.3$ , close to the value of  $\sim 7.2$  previously reported in (3), although the absolute numbers differ, as discussed above. Note that a downward reevaluation of  $\text{CH}_4$  emissions from tropical lakes could contribute to partly close the gap of global  $\text{CH}_4$  emission estimates based on the top-down approach (modeled from observations of atmospheric  $\text{CH}_4$ ) and bottom-up approach (extrapolation per ecosystem of discrete flux estimates) (33).

Compared with previous reports, the integrated  $F\text{CO}_2$  was 11 times lower for tropical African lakes ( $3.3 \pm 1.0$   $\text{TgC year}^{-1}$ ) and between 6 and 25 times lower for pan-tropical lakes ( $17.5 \pm 9.1$   $\text{TgC year}^{-1}$ ; Table 1 and table S4). The previously published  $\text{CO}_2$  emission for large tropical lakes only (surface area larger than 500  $\text{km}^2$ ) of 5.4  $\text{TgC year}^{-1}$  (27) was also marginally higher than our own estimate for the same lake size class of  $3.3 \pm 1.7$   $\text{TgC year}^{-1}$ . This is related to the fact that  $F\text{CO}_2$  per square meter was low or even negative in nonhumic lakes, although  $F\text{CO}_2$  per square meter in humic lakes was similar to previous estimates (table S4). The  $p\text{CO}_2$  values that we scaled were much lower than previously reported, between 1.8 and 4.3 times for African lakes and  $\sim 2.3$  for pan-tropical lakes (table S4).

Integrated diffusive  $F\text{CH}_4$  from African lakes ( $0.4 \pm 0.1$   $\text{TgCH}_4 \text{ year}^{-1}$ ) was lower than that from African rivers ( $\sim 4.5$   $\text{TgCH}_4 \text{ year}^{-1}$ ) (34).  $F\text{CO}_2$  from African lakes (6  $\text{TgC year}^{-1}$ ) was also distinctly lower than that from African rivers ( $\sim 300$   $\text{TgC year}^{-1}$ ) (34). We conclude that African inland water  $\text{CO}_2$  and  $\text{CH}_4$  emissions are mainly lotic despite the fact that the total surface area of rivers and streams in Africa (68,560  $\text{km}^2$ ) is distinctly lower than that of tropical lakes (209,394  $\text{km}^2$ ). At the pan-tropical scale, lentic  $F\text{CO}_2$  was also lower (18  $\text{TgC year}^{-1}$ ) than lotic  $F\text{CO}_2$  ( $\sim 1800$   $\text{TgC year}^{-1}$ ) (35).

A large contribution to inland water  $\text{CO}_2$  and  $\text{CH}_4$  emissions from small water bodies (ponds) has been recently suggested (26)

on the basis of data mainly collected in boreal systems ( $\sim 190$ ) and in a limited number of temperate systems ( $\sim 40$ ) but with no data for tropical systems. Small lakes, at tropical African and pan-tropical scales, were much more abundant than large lakes, although the relative surface area increased with lake size (Fig. 9). The relative surface area of large lakes ( $>1000$   $\text{km}^2$ ) compared to the total was higher at the African scale (86%) than at the pan-tropical scale (63%). For humic African tropical lakes,  $F\text{CO}_2$ , diffusive  $F\text{CH}_4$ , and  $\text{FN}_2\text{O}$  regularly increased with lake size area (Fig. 9). In pan-tropical humic lakes,  $F\text{CH}_4$ ,  $F\text{CO}_2$ , and  $\text{FN}_2\text{O}$  were more evenly distributed among size classes. For nonhumic lakes, diffusive  $F\text{CH}_4$  tended to increase with lake size both at African and pan-tropical scales. For nonhumic lakes both at African and pan-tropical scales, the sink of atmospheric  $\text{CO}_2$  increased with lake size but reverted to a source of  $\text{CO}_2$  to the atmosphere for the largest size class. For nonhumic African and pan-tropical lakes, the sink of atmospheric  $\text{N}_2\text{O}$  also increased with lake size until the largest size class, for which the  $\text{N}_2\text{O}$  atmospheric sink decreased (Fig. 9).

### Uncertainties in the computation and integration of GHG fluxes

Our strategy of data acquisition aimed first to describe interlake variations of GHG concentrations and, secondly, to describe the intralake spatial variations in the subset of the largest lakes (Victoria, Tanganyika, Albert, Kivu, and Edward). Consequently, the temporal variability was less constrained, particularly with regard to daily variations, since data were only acquired during daytime, as well as to seasonal variations, since lakes were only sampled repeatedly a few times (table S7).

Admittedly, diel variations were not represented explicitly in our estimates of  $\text{CO}_2$  and  $\text{CH}_4$  emissions from African lakes, but this should not radically change our overall conclusions that nonhumic lakes were low  $\text{CO}_2$  sources or even sinks of atmospheric  $\text{CO}_2$ . We compared  $p\text{CO}_2$  at dusk and dawn during the three cruises in Lake Victoria, and in only 11% of the comparisons of maximum diel amplitude of  $p\text{CO}_2$  change (dusk-dawn difference) was there a change in the sign of  $\Delta p\text{CO}_2$  (direction of the flux) (fig. S11). In addition, the fact that data were mainly acquired during daytime should not have substantially underestimated the  $\text{CO}_2$  emission rates because of supposedly much higher emission values during nighttime. On the contrary, diel measurement cycles in Lakes Kivu and Edward show that daytime  $\text{CO}_2$  emissions were higher than nighttime because of higher daytime wind speed (fig. S12). This seemed to be a general feature in Lakes Victoria, Tanganyika, Kivu, and Edward (fig. S13). Furthermore, all previous estimates of  $\text{CO}_2$  emissions from tropical lakes were presumably also based on daytime observations and did not account for the diel variations. Together, our conclusion that  $\text{CO}_2$  emission estimates from tropical lakes are lower than those from previous studies remains valid. Daytime diffusive  $\text{CH}_4$  emissions could be higher than nighttime values, possibly because of the photoinhibition of MOX (22), leading to higher  $\text{CH}_4$  concentrations during daytime (also based on dusk-dawn comparisons of  $\text{CH}_4$  in Lake Victoria; fig. S14) and higher daytime wind speed and  $k$  (fig. S13). Note that the difference between night- and daytime of  $\text{CH}_4$  concentration inferred from dusk-dawn comparisons in Lake Victoria (fig. S14) was modest (median of  $-6$  nM; range of  $-200$  and 97 nM) compared to the range of spatial variations observed within Lake Victoria itself (3 to 911 nM; Fig. 4), as well as the range of  $\text{CH}_4$  values across different lakes (19 to 490,749 nM; Fig. 2).

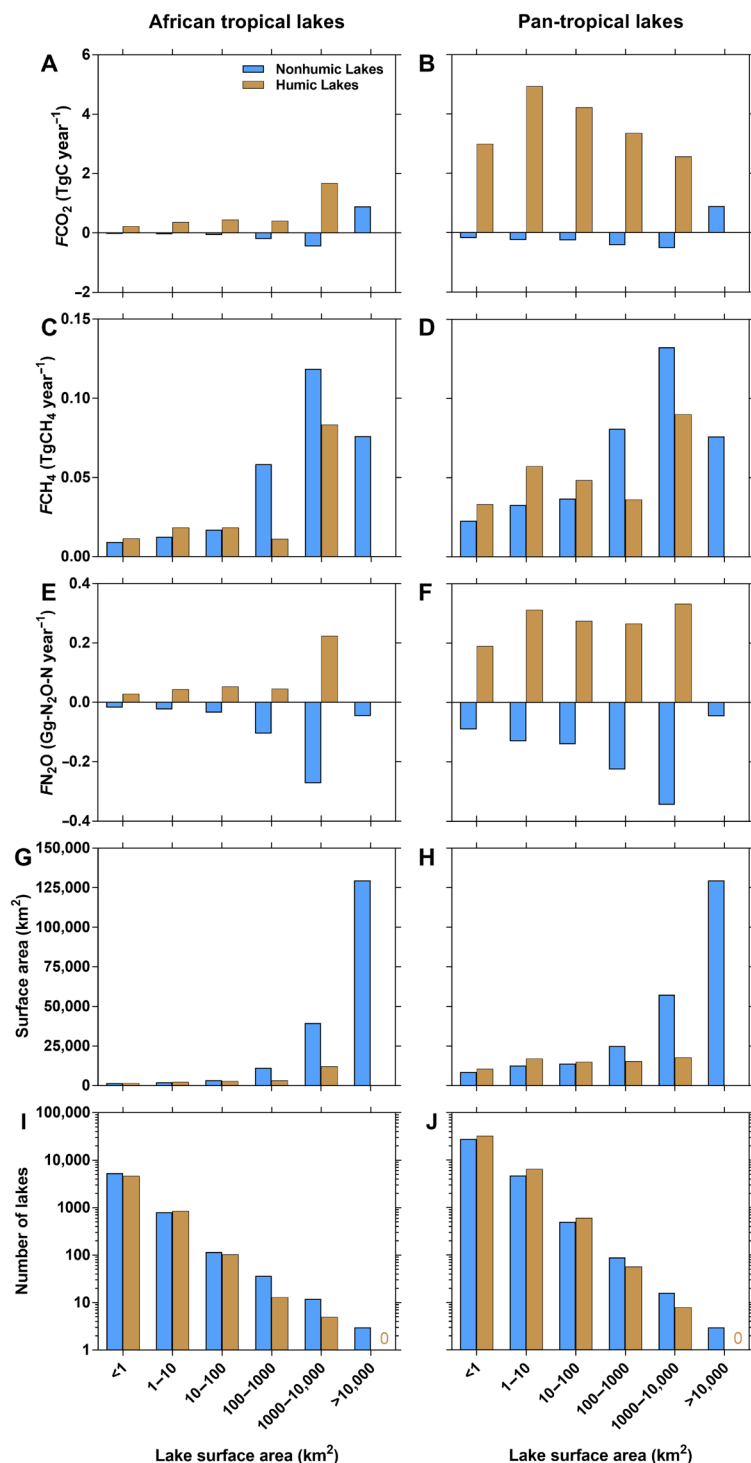


**Fig. 9. Large contribution to  $\text{CO}_2$ ,  $\text{CH}_4$ , and  $\text{N}_2\text{O}$  emissions from very large lakes.** Air-water flux of  $\text{CO}_2$  ( $F_{\text{CO}_2}$ ),  $\text{CH}_4$  ( $F_{\text{CH}_4}$  diffusive), and  $\text{N}_2\text{O}$  ( $F_{\text{N}_2\text{O}}$ ) integrated for African tropical (A, C, and E) and pan-tropical lakes (B, D, and F) that were classified into humic and nonhumic, as well as surface area (G and H) and number of lakes per size classes (I and J) from HydroLAKES (29), except for Lake Chad for which the more recent and realistic surface area was applied (30).

Five lakes (Victoria, Tanganyika, Kivu, Edward, and George) were repeatedly sampled (table S7), allowing us to describe the amplitude of seasonal variations (fig. S15). The amplitude of seasonal variations of  $\text{CH}_4$  was much stronger in shallower waters and more pronounced in holomictic compared to meromictic lakes. Moreover,

they followed the pattern of depth dependence of productivity as indicated by average Chl-a (fig. S15). Seasonal variations of  $\text{pCO}_2$  were lower in the meromictic Lake Tanganyika and generally small and equivalent for all the other lakes, except for Lake Victoria, where seasonal  $\text{pCO}_2$  changes were particularly strong. Seasonal variations

of  $p\text{CO}_2$  in surface waters were attributable to the alternation of periods of vertical mixing and transport to surface of  $\text{CO}_2$  from depth and periods of stratification with a decrease of  $\text{CO}_2$  content in surface waters due to primary production. At an equivalent depth (30 m), the vertical gradients of  $p\text{CO}_2$  were much stronger in Lake Victoria than in Lake Edward (fig. S16), explaining the corresponding higher amplitude of  $p\text{CO}_2$  seasonal variations in Lake Victoria compared to Lake Edward (fig. S15). To derive GHG concentrations representative for each lake, before scaling of fluxes, we simply averaged all sampling periods for lakes Tanganyika, Kivu, Edward, and George where seasonal variations were small (fig. S15), while for Lake Victoria, the annual average was computed using a period of 2 months for the mixed conditions and period of 10 months for the stratified conditions (36).

The reliability of pan-tropical integration of GHGs partly depends on degree to which GHG data collected in African lakes are representative for tropical lakes in other continents. For  $\text{CH}_4$ , data collected in tropical lakes in other regions than Africa were generally comparable and consistent with the patterns in African lakes as a function of depth and surface area (fig. S17). This was also the case for  $p\text{CO}_2$  in nonhumic lakes (fig. S18). Regarding humic lakes,  $p\text{CO}_2$  collected in Amazonian floodplain lakes were comparable to data in African humic lakes for larger systems (surface area,  $>260 \text{ km}^2$ ) but higher for smaller systems (surface area,  $<260 \text{ km}^2$ ) (fig. S19). The fact that the difference was size dependent is probably attributable to the Amazonian floodplain lakes having a very strong hydrological connectivity with the Amazon River; during the high-water period, these floodplain lakes are entirely filled by river water with a very high  $\text{CO}_2$  content and only become hydrological disconnected from the river during the low water period. The computation of the  $F\text{CH}_4$  and  $F\text{CO}_2$  at pan-tropical scale included the data from non-African tropical lakes (figs. S17 to S19). Note that median  $p\text{CO}_2$  measured directly by equilibration in Amazon floodplain lakes (fig. S19) of 2880 ppm (IQR: 1752 to 3380,  $n = 14$ ) was distinctly lower than median  $p\text{CO}_2$  in Amazonian lakes calculated from pH and TA of 4860 ppm (IQR: 3858 to 9636,  $n = 11$ ) reported in (37) and 8260 ppm (IQR: 3200 to 12,800,  $n = 65$ ) reported in (9). These differences might be related to a systematic overestimation of  $p\text{CO}_2$  computed from pH and TA in humic waters (28).

We tested three alternative scaling procedures for  $F\text{CO}_2$  for African lakes since the  $F\text{CO}_2$  estimates that we provide strongly diverge from previously published ones, unlike  $F\text{CH}_4$  for which there is relatively more convergence (Table 1 and table S8). First, we simply upscaled the surface area-weighted average  $\Delta p\text{CO}_2$  of 12 ppm of all 25 lakes. A surface area-weighted average seemed more adequate than a simple average since the lake surface area in our dataset spans five orders of magnitude (table S1). This provided an integrated  $F\text{CO}_2$  for African lakes of  $0.3 \text{ TgC year}^{-1}$ , about 11 times lower than our nominal estimate (Table 1), because of a predictable strong underestimation of the  $\text{CO}_2$  emission from humic lakes since the largest lakes were nonhumic and have the strongest weight on the average. This supports our choice to separate humic and nonhumic lakes in our nominal scaling. Second, we used a  $\Delta p\text{CO}_2$  versus DOC relation (table S8) that was applied to a dataset of DOC calculated with a statistical model (38) for the lakes included in HydroLAKES (29). This predicted that African lakes acted collectively as a sink of atmospheric  $\text{CO}_2$  of  $-4.2 \text{ TgC year}^{-1}$  because of a strong underestimation of the modeled DOC values compared to the measured DOC in the African lakes (fig. S20). The model seems to account

realistically neither for autochthonous DOC inputs in productive nonhumic lakes nor for lateral inputs of DOC from wetlands in humic lakes (fig. S20). Third, we used a relation between  $\Delta p\text{CO}_2$  and lake surface area by separating humic and nonhumic lakes, although the relationship was positive for both lake types (table S8). This provided an integrated  $F\text{CO}_2$  for African lakes of  $5.7 \pm 1.7 \text{ TgC year}^{-1}$  (table S8), higher but still relatively close to our nominal estimate of  $3.3 \pm 1.0 \text{ TgC year}^{-1}$  (Table 1). The positive relation between  $\Delta p\text{CO}_2$  and surface area in humic lakes was driven by the two largest lakes (Mai Ndombe and Tumba) that coincidentally were located in the Cuvette Centrale Congolaise, a giant wetland in the Congo basin that provides very high amounts of organic and inorganic carbon to streams (17). A positive relation between  $p\text{CO}_2$  and surface area is in itself counterintuitive, as hydrological connectivity with wetlands and the rest of the catchment, and consequently lake  $\text{CO}_2$  content, should be stronger in smaller water bodies (fig. S4), as also indicated by the comparison with Amazonian floodplain lakes (fig. S19). Our nominal estimate based on the scaling of the median  $\Delta p\text{CO}_2$  for humic lakes seems more robust given the low number of observations and clearly calls for more observations of GHGs dynamics in tropical humic lakes, which, in the future, should allow more elaborate scaling procedures.

A final additional possible limitation of our scaling approach is that HydroLAKES includes only lakes with a surface area larger than  $0.1 \text{ km}^2$ . Statistical extrapolations predict that lakes smaller than  $0.1 \text{ km}^2$  are extremely numerous, yet they might only contribute marginally to total limnetic area based on an analysis of high-resolution satellite imagery (39).

The summed lake surface area of sampled African lakes (including Lake Malawi) accounts for 63% of the total tropical African lacustrine surface area that, in turn, accounts for 66% of the total surface area of tropical lakes larger than  $0.1 \text{ km}^2$  (29), giving confidence in our pan-tropical scaling. We included in the scaling procedure a large-scale classification and separate scaling of humic and nonhumic lakes that seemed essential given the very different behavior of  $\text{CO}_2$  and  $\% \text{N}_2\text{O}$  in these two types of lakes and is in line with the idea that CDOM is a major factor controlling lake productivity and overall carbon cycling (12). Also in line with the idea that depth controls to a large extent productivity in lakes (15), we used relations between  $p\text{CO}_2$  and lake morphology (depth), which should improve previous scaling efforts based on the simple extrapolation of the median of available values (4).

In recent literature, there is an inflationary tendency to publish increasingly higher  $\text{CO}_2$  emissions from inland waters, the latest values (40) up to  $\sim 5000 \text{ TgC year}^{-1}$ , distinctly higher than earlier estimates of  $\sim 700 \text{ TgC year}^{-1}$  (41). This might be unreasonable because  $\text{CO}_2$  emissions from inland waters should be sustained by external carbon inputs, assumed to be provided by the terrestrial biosphere (41). It is becoming increasingly difficult to reconcile such high inland water  $\text{CO}_2$  emissions with independent estimates of hydrological export of inorganic and organic carbon from land, given by the terrestrial science community. This hydrological export of  $\text{CO}_2$  and DOC from soils to rivers is computed as a fraction of terrestrial net ecosystem exchange (NEE) defined as the difference between gross  $P$  and net ecosystem  $R$  (sum of autotrophic and heterotrophic  $R$  components) and is reported to vary between 3% for forests and 13% for grasslands (42). NEE as defined here differs from the long-term storage of carbon in terrestrial ecosystems, commonly called net biome production, corresponding to NEE

minus all the other losses of dead or living organic matter such as harvest, forest clearance, fire, and leaching of carbon to inland waters. Global grassland NEE is low (43), so assuming that the majority of carbon hydrological export is from forests (3% of NEE) (42), it should sustain a CO<sub>2</sub> emission of ~400 TgC year<sup>-1</sup>, based on the terrestrial NEE of ~20,000 TgC year<sup>-1</sup> (44) and also taking into account the export of DOC from rivers to the ocean of ~200 TgC year<sup>-1</sup> (45). A way to address this large discrepancy and reconcile these independent estimates is to attribute a large part of CO<sub>2</sub> emissions from rivers to carbon inputs from wetlands rather than from “dry” terrestrial catchments, particularly in the tropics (17, 34, 35), as hydrological export of CO<sub>2</sub> and DOC from wetlands to inland waters is much higher than from dry land (46). In addition, there might be a need to reevaluate downward the global CO<sub>2</sub> emissions from inland waters, and this seems to be the case for tropical lakes, as shown here. This might also require challenging the longstanding paradigm of lakes as nearly universal sources of CO<sub>2</sub> sustained by prevailing net heterotrophy (41), as also shown here (Fig. 5).

## MATERIALS AND METHODS

We focus exclusively on natural lakes, although we acquired data in five reservoirs in Zambia and Kenya that have been reported elsewhere (51, 52). Natural lakes and reservoirs need to be treated separately, as the CO<sub>2</sub> and CH<sub>4</sub> emissions from reservoirs are sustained by the drowned former terrestrial biomass and strongly evolve with reservoir age (53). In addition, reservoirs only represent <13% of the surface area of lentic water bodies in Africa given by Hydro-LAKES (29). The sampled lakes can be considered as near-pristine, except Lake Victoria where the nearshore areas and bays are strongly eutrophicated, although a recent decrease since the 1990s in phytoplankton biomass has been reported (54).

### Field sampling

We measured dissolved concentrations of CH<sub>4</sub> on 297 samples, N<sub>2</sub>O on 241 samples, and pCO<sub>2</sub> on 287 samples collected in surface waters of 24 African lakes from 2007 to 2021 (table S7). The CO<sub>2</sub> and CH<sub>4</sub> data from four cruises in Lake Kivu were previously reported (49, 55). All of the variables reported in this study were obtained with the same sampling and analytical protocols, providing a dataset that is methodologically consistent and of uniform quality. Sampling was done from small boats (fishermen boats or own inflatable boat) or larger ships for the two largest lakes (*Maman Benita* in Lake Tanganyika and *RV Hammerkop* in Lake Victoria). In small lakes, data were only acquired at one location (typically in the deepest central part of the lake), while in larger lakes, sampling was done at several locations, covering the depth gradient from the littoral zone to the deepest part of the lake. Sampling was done during daytime, from dawn to dusk in the case of continuous surface measurements in Lakes Victoria and Tanganyika, and typically from early morning to mid-afternoon in other lakes.

### Sample handling and analysis

Depth at the sampling point was measured with a portable echosounder (Plastimo Echotest-II or Humminbird Helix 5 G2). Water temperature, conductivity, pH, and dissolved O<sub>2</sub> were measured with Yellow Springs Instrument (YSI) multiprobes (YSI 6600, YSI Pro Plus, and YSI EXO-2). The dissolved gases were measured with a uniform method based on a head-space technique, either directly

in the field by infrared gas analysis (LI-COR Li-840 for CO<sub>2</sub>) or upon return in the laboratory by gas chromatography (GC; for CH<sub>4</sub> and N<sub>2</sub>O). Water was collected with a Niskin bottle below the surface (<0.5 m), and two 60-ml borosilicate serum bottles (Wheaton) for the determination of CH<sub>4</sub> and N<sub>2</sub>O were filled with a silicone tubing, allowed to overflow, poisoned with a saturated solution of HgCl<sub>2</sub> (100 µl), sealed with butyl stoppers, crimped with aluminum caps, and stored at ambient temperature in the dark (34). Samples for the determination of pCO<sub>2</sub> were collected from the Niskin bottle in four 60-ml polypropylene syringes where 30 ml of sample water was equilibrated with 30 ml of ambient air (5 min of vigorous manual shaking) (34). The pCO<sub>2</sub> in ambient air and in the equilibrated gas phase was determined with a Li-840 calibrated with N<sub>2</sub> and a suite of CO<sub>2</sub>:N<sub>2</sub> commercial mixtures (Air Liquide Belgium) with mixing ratios of 388-, 813-, 3788-, and 8300-ppm CO<sub>2</sub>. The overall precision of pCO<sub>2</sub> measurements was ±2.0%. Concentrations of CH<sub>4</sub> and N<sub>2</sub>O were determined via the headspace equilibration technique (20-ml N<sub>2</sub> headspace in 60-ml serum bottles) and measured by GC with flame ionization detection (GC-FID) and electron capture detection (GC-ECD) with an SRI 8610C GC-FID-ECD calibrated with CH<sub>4</sub>:CO<sub>2</sub>:N<sub>2</sub>O:N<sub>2</sub> mixtures (Air Liquide Belgium) of 1-, 10-, 30-, 509-, and 2011-ppm CH<sub>4</sub> and of 0.2-, 2.0-, and 6.0-ppm N<sub>2</sub>O and using the solubility coefficients of CH<sub>4</sub> (56) and N<sub>2</sub>O (57). The precision of measurements was ±3.9% for CH<sub>4</sub> and ±3.2% for N<sub>2</sub>O. During six cruises in Lakes Victoria, Tanganyika, Edward, and Albert (fig. S21), we also measured pCO<sub>2</sub> and the partial pressure of CH<sub>4</sub> (pCH<sub>4</sub>) with a Los Gatos Research (LGR) off-axis integrated cavity output spectroscopy analyzer (Ultraportable Greenhouse Gas Analyzer with extended range for CH<sub>4</sub>) coupled to an equilibrator. The reading of pCO<sub>2</sub> and pCH<sub>4</sub> from the LGR was compared in the home laboratory to the values from CH<sub>4</sub>:CO<sub>2</sub>:N<sub>2</sub> mixtures (Air Liquide Belgium) of 1-, 10-, 30-, 509-, and 2011-ppm CH<sub>4</sub> and 431-, 1088-, 4385-, and 22,029-ppm CO<sub>2</sub>. The instrument did not show detectable drift between the start and the end of the fieldwork, and the factory calibration gave satisfactory readings against standards. This allowed a total of 29,127 surface measurements of pCO<sub>2</sub> and CH<sub>4</sub> (table S7). During these cruises, the pCO<sub>2</sub> and CH<sub>4</sub> were also measured with a headspace technique and measured with an infra-red gas analyzer (IRGA) and GC, respectively, on samples collected with a Niskin bottle. These measurements were consistent with the measurements obtained with the LGR analyzer coupled to the equilibrator (fig. S22). In Lake Edward, continuous unattended measurements of pCO<sub>2</sub> were carried out for 45 hours (fig. S12) using a custom-made equilibration system mounted on a floater inspired from (58) incorporating a Senseair ELG CO<sub>2</sub> analyzer.

Samples for δ<sup>13</sup>C-DIC were collected from the Niskin bottle with a silicone tube in 12-ml Exetainer vials (Labco) and poisoned with 50 µl of a saturated solution of HgCl<sub>2</sub>. Measurements were made with an elemental analyzer–isotope ratio mass spectrometer (Thermo FlashHT or Carlo Erba EA1110 with DeltaV Advantage). Calibration was performed with certified standards (NBS-19 or IAEA-CO-1, and LSVEC). Reproducibility of measurement based on duplicate injections of samples was typically better than ±0.2 ‰.

Water was filtered on Whatman glass fiber filters (GF/F grade; porosity, 0.7 µm; diameter, 47 mm) for phytoplankton pigments analyzed on 90% acetone extracts by high-performance liquid chromatography (HPLC) with a Waters HPLC chain (fluorescence and photodiode detectors), with a reproducibility for Chl-a of ±0.5% and a detection limit of 0.01 µg liter<sup>-1</sup>. The abundance of

phytoplankton classes including the cyanobacteria was derived with CHEMTAX (59).

The water filtered through GF/F Whatman glass fiber filters was collected and further filtered through polyethersulfone syringe encapsulated filters (porosity, 0.2  $\mu\text{m}$ ) for samples to DOC, CDOM,  $\text{NO}_3^-$ ,  $\text{NO}_2^-$  and  $\text{NH}_4^+$ , and TA. Samples to determine DOC were stored at 4°C and in the dark in 40-ml brown borosilicate vials with polytetrafluoroethylene (PTFE)-coated septa and poisoned with 50  $\mu\text{l}$  of  $\text{H}_3\text{PO}_4$  (85%), and DOC concentration was determined with a wet oxidation total organic carbon analyzer (IO Analytical Aurora 1030W), with a typical reproducibility better than  $\pm 5\%$ . Samples to determine CDOM were stored at 4°C and in the dark in 20-ml brown borosilicate vials with PTFE-coated septa. Absorbance spectra were measured from 190 to 900 nm at 1-nm increments with a PerkinElmer UV/Vis 650S spectrophotometer using a 1-cm quartz cuvette, and SR was computed according to the work in (11). Samples for the determination of  $\text{NO}_3^-$ ,  $\text{NO}_2^-$ , and  $\text{NH}_4^+$  were collected in 50-ml polypropylene vials and stored frozen ( $-20^\circ\text{C}$ ).  $\text{NO}_3^-$  and  $\text{NO}_2^-$  were determined with the sulfanilamide colorimetric with the vanadium reduction method (60), and  $\text{NH}_4^+$  with the dichloroisocyanurate-salicylate-nitroprussiate colorimetric method (61). Detection limits were 0.3, 0.01, and 0.15  $\mu\text{M}$  for  $\text{NH}_4^+$ ,  $\text{NO}_2^-$ , and  $\text{NO}_3^-$ , respectively. Precisions were  $\pm 0.02$ ,  $\pm 0.02$ , and  $\pm 0.1$   $\mu\text{M}$  for  $\text{NH}_4^+$ ,  $\text{NO}_2^-$ , and  $\text{NO}_3^-$ , respectively. Samples for TA were stored at ambient temperature in 55-ml polyethylene vials, and measurements were carried out by open-cell titration with 0.1 M HCl, and data were quality checked with certified reference material obtained from Andrew Dickson (Scripps Institution of Oceanography, University of California, San Diego, CA, USA), with a typical reproducibility better than  $\pm 3$   $\mu\text{mol kg}^{-1}$ .  $\text{HCO}_3^-$  was computed from TA and  $\text{pCO}_2$  measurements using the carbonic acid dissociation constants for freshwater and the CO2SYS package.

$P$  was measured during 2-hour incubations along a gradient of light intensity using  $^{13}\text{C-HCO}_3^-$  as a tracer, as described in detail elsewhere (22). For Lake Mai Ndombe,  $P$  was calculated with a statistical model using Secchi disk depth and Chl-*a* concentration developed for the Congo River network (17). Pelagic community  $R$  was determined from the decrease of  $\text{O}_2$  measured with an optical  $\text{O}_2$  probe (YSI ProODO) in 60-ml biological oxygen demand bottles (Wheaton) over  $\sim 24$ -hour incubation periods (17).

### Air-water flux computation and upscaling

The general approach to scale  $F\text{CO}_2$ ,  $F\text{CH}_4$ , and  $F\text{N}_2\text{O}$  for tropical lakes (24°N to 24°S) at African and pan-tropical scales was as follows: (i) classification of lakes in HydroLAKES into humic and nonhumic lakes based on wetland coverage derived from GIEMS-D15 (62); (ii) computation of air-water  $\text{CO}_2$ ,  $\text{N}_2\text{O}$ , and  $\text{CH}_4$  concentration gradients based on relations with lake mean depth for each lake in HydroLAKES (29), using two different approaches for humic and nonhumic lakes (for  $\text{CO}_2$  and  $\text{N}_2\text{O}$ ); (iii) computation of  $F\text{CO}_2$ ,  $F\text{N}_2\text{O}$ , and  $F\text{CH}_4$  fluxes per square meter from the respective air-water concentration gradients, water temperature [derived for each lake from a relation with air temperature derived from WorldClim (63)], and the  $k$  computed from a parameterization as a function of wind speed (64) itself derived for individual lakes in HydroLAKES from WorldClim (63); and (iv) integration of the fluxes from fluxes per square meter for each lake and the respective surface area from HydroLAKES (29). Two versions of the scaling were made: one using the original HydroLAKES surface area data with an unrealistic

surface area value of 18,752  $\text{km}^2$  for Lake Chad and another using a more recent surface area value of 2603  $\text{km}^2$  for Lake Chad (30).

HydroLAKES (29) is a global database of lake morphology for lakes with a surface area  $\geq 0.1$   $\text{km}^2$ , which incorporates lake mean depth. We classified the objects in HydroLAKES for natural lakes (unregulated, category 1; regulated, category 3; excluding reservoirs, category 2) into strongly humic lakes and nonhumic lakes. We hypothesized that wetlands fringing lakes were the major source of humic DOM to the lakes, and CDOM SR was negatively correlated with wetland presence on the catchment extracted from GIEMS-D15 (62). On the basis of the regression of CDOM SR as a function of % wetland

$$\text{CDOM SR} = 1.85 - 0.0765 \times \% \text{wetland} \quad (r^2 = 0.57, P = 0.0003, n = 18).$$

We computed the threshold value of wetland coverage of 8.1% to classify humic (CDOM SR < 1) and nonhumic (CDOM SR > 1) lakes. For each lake in HydroLAKES, the watershed was extracted from HydroSHEDS (65) allowing us, in turn, to extract the wetland coverage on the watershed from GIEMS-D15 (62). GIEMS-D15 data were unavailable for 707 tropical lakes totaling a surface area of 395  $\text{km}^2$  ( $\sim 0.1\%$  of total) of which 92 lakes in the African continent totaling a surface of 29  $\text{km}^2$  ( $\sim 0.01\%$  of total), and these lakes were excluded from the analysis. While this approach is admittedly coarse, it is a first attempt to classify lakes into humic and non-humic classes that have been shown to be important in driving  $\text{CO}_2$  concentrations rather than simply extrapolating a central value of  $\text{CO}_2$  concentration either globally (1, 2) or zonally (4). In addition, the general approach is conceptually consistent with the independent evidence showing that the presence of wetlands is important in sustaining high  $\text{CO}_2$  concentrations in temperate and boreal lakes (13, 66).

The annual average of both the wind speed and the air temperature was also extracted for each lake from WorldClim (63). The surface lake water temperature was computed from air temperature using a linear regression as a function of the latitude of the difference of air and water temperature in 76 tropical lakes from a recent global compilation (fig. S23) (67)

$$\text{Air temperature} - \text{water temperature} = 0.1001 * \text{LAT} - 3.66 \quad (n = 76; r^2 = 0.2; P < 0.0001)$$

where LAT is absolute latitude (in degrees).

The derived lake surface temperature compared satisfactorily to our average measured data, except for two of the warmest lakes (fig. S24). Excluding these two outliers, the root mean square value was  $\pm 1.3^\circ\text{C}$ .

For large lakes where data distribution covered a depth gradient (Albert, Edward, Tanganyika, and Victoria), the GHG data were binned by depth and the average for the whole lake was calculated from bathymetry maps. For Lakes Edward and Albert, bathymetry was digitized from (68); for Lake Tanganyika, digital bathymetry was provided by TCarta, and for Lake Victoria, bathymetry was available from (69). For the lakes where sampling was obtained during various cruises, the spatially integrated averages based on bathymetry were averaged to provide an annual mean. The period of different cruises were chosen to cover contrasted periods of the year in terms of vertical mixing that typically follow the alternation of the rainy and the dry seasons. The seasonal variations tended to be relatively modest in most lakes, except for Lake Victoria that showed much higher  $\text{pCO}_2$  values during the cruise during the dry season when vertically mixed conditions were observed (54)

compared to two other cruises when stratified condition prevailed (54). For Lake Victoria, we then averaged the data considering that the period of vertical mixing lasted 2 months (36) and stratified conditions lasted 10 months per year.

For nonhumic African lakes,  $\Delta p\text{CO}_2$  and  $\% \text{N}_2\text{O}$  were computed from lake mean depth according to

$$\Delta p\text{CO}_2 = 147.3 \times \log(\text{mean depth}) - 250.3 \quad (r^2 = 0.29, P = 0.0399, n = 15)$$

$$\% \text{N}_2\text{O} = 18.321 \times \log(\text{mean depth}) + 55.4 \quad (r^2 = 0.30, P = 0.0153, n = 19)$$

The same relation between  $\% \text{N}_2\text{O}$  and mean depth was used for the pan-tropical lake upscaling (in the absence of additional  $\text{N}_2\text{O}$  data in other tropical lakes), but for  $\Delta p\text{CO}_2$ , we added two data points (fig. S18) for the pan-tropical nonhumic lake upscaling, according to

$$\Delta p\text{CO}_2 = 133.41 \times \log(\text{mean depth}) - 231.5 \quad (r^2 = 0.24, P = 0.0446, n = 17)$$

For humic lakes, there was no relation between  $\Delta p\text{CO}_2$  and  $\% \text{N}_2\text{O}$  and lake mean depth, so we used the median  $\Delta p\text{CO}_2$  value of 1302 ppm and the median  $\% \text{N}_2\text{O}$  value of 167.2%. The same median of  $\% \text{N}_2\text{O}$  value was used for the pan-tropical humic lake upscaling (in the absence of additional  $\text{N}_2\text{O}$  data in other tropical lakes). For the pan-tropical upscaling of  $F\text{CO}_2$  in humic lakes, we included 14 additional data points from Amazon floodplain lakes (fig. S19), and we used a median  $\Delta p\text{CO}_2$  of 2657 ppm for lakes  $< 260 \text{ km}^2$  and a median  $\Delta p\text{CO}_2$  of 1373 ppm for lakes  $> 260 \text{ km}^2$ .

No clear differences in  $\text{CH}_4$  concentration as a function of depth was observed between humic and nonhumic lakes, so a single overall relation was applied to all African lakes

$$\log(\text{CH}_4) = -0.6226 \times \log(\text{mean depth}) + 3.29 \quad (r^2 = 0.18, P = 0.0391, n = 24)$$

For the pan-tropical upscaling, we included 35 additional  $\text{CH}_4$  data points (fig. S17) using the following relation

$$\log(\text{CH}_4) = -0.4123 \times \log(\text{mean depth}) + 2.807 \quad (r^2 = 0.12, P = 0.0086, n = 59)$$

The flux ( $F$ ) of GHGs between surface waters and the atmosphere was computed according to

$$F = k \cdot \Delta G$$

where  $k$  is the gas transfer velocity (centimeters per hour) and  $\Delta G$  is the air-water gradient of dissolved concentration of a given gas.

We computed  $k$  for each lake in HydroLAKES as a function of wind speed using a parameterization based on the compilation of tracer-based estimates of  $k$  in 11 lakes with a wide range of morphological characteristics such as maximum depth (Dozmary pool, 0.7 m; Pyramid lake, 109 m) and surface area (Dozmary pool, 0.14  $\text{km}^2$ ; Pyramid lake, 487  $\text{km}^2$ ) (64). While  $k$  is parameterized as a function of wind speed, this does imply that this parameterization only accounts for the effect on  $k$  of turbulence generated by wind shear. This parameterization intrinsically integrates at least partly other sources of turbulence such as convection due to nighttime cooling (70) or the modulation of  $k$  by fetch limitation (16, 71) because the parameterization is built on compilation of numerous tracer measurements (lasting typically 1 to 2 weeks) in several lakes covering a wide range of size and depth, thus integrating all the drivers of  $k$  in lakes. In lakes,  $k$  is known to show a fetch dependence that seems to be a function of lake surface area (16, 71), which has led to the use of a constant  $k$  with a different value for several lake size classes to scale  $\text{CO}_2$  fluxes globally in lakes (4). The  $k$  value specific to each lake size class was calculated from the compilation of  $k$  values

derived from tracer experiments in temperate or boreal systems (4). However, wind speed is zonally variable as a function of latitude, with tropical landmasses showing distinctly lower values than higher-latitude areas (fig. S25). Consequently, the area-averaged  $k$  based on the  $k$ -wind relationship (64) that we computed and used in the scaling was about 1.6 times lower than the  $k$  values computed from the  $k$ -surface area classes tabulated in (4) both at tropical African (3.0  $\text{cm hour}^{-1}$  versus 4.7  $\text{cm hour}^{-1}$ ) and pan-tropical (2.9  $\text{cm hour}^{-1}$  versus 4.6  $\text{cm hour}^{-1}$ ) scales. The pan-tropical area-averaged  $k$  based on the  $k$ -wind relationship (2.9  $\text{cm hour}^{-1}$ ) (64) was also lower than the one used in (47) (4.0  $\text{cm hour}^{-1}$ ), although there is no indication in (47) on how this average value was derived.

Error analysis on the GHG flux computation and upscaling was carried out by error propagation of the GHG concentration measurements, the  $k$  value estimates, and the classification into humic and nonhumic lakes using a Monte Carlo simulation with 10,000 iterations. The uncertainty on  $p\text{CO}_2$ ,  $\text{CH}_4$ , and  $\text{N}_2\text{O}$  was arbitrarily set at  $\pm 25\%$  to account for the uncertainty arising from the representativeness of available data to capture all spatial and temporal scales of variability and also including the uncertainty of measurements of  $\pm 2.0\%$  for  $p\text{CO}_2$ ,  $\pm 3.9\%$  for  $\text{CH}_4$ , and  $\pm 3.2\%$  for  $\text{N}_2\text{O}$ . The uncertainty on  $k$  derived from tracer experiments was evaluated to  $\pm 30\%$  on the basis of the reported (64) variability across different lakes of  $k$  at low wind speeds, characteristic of low-latitude land masses (fig. S25). The uncertainty on the lake surface temperature was  $\pm 1.3^\circ\text{C}$  (fig. S24). The uncertainty on the classification into humic and nonhumic lakes was arbitrarily set at  $\pm 25\%$ .

Ebullitive  $F\text{CH}_4$  was scaled for both humic and nonhumic lakes using a median of 5.7 (IQR: 2.1 to 14.6)  $\text{mmol m}^{-2} \text{day}^{-1}$  for the littoral zone between depth of 0 and 4 m and a median of 5.2 (IQR: 1.7 to 8.7)  $\text{mmol m}^{-2} \text{day}^{-1}$  for the littoral zone between 4 and 10 m derived from a compilation of 23 data in tropical lakes including our own four measurements in African lakes (fig. S10). This was motivated by the fact that ebullitive  $F\text{CH}_4$  shows a strong depth dependence and is usually confined to shallow depths in boreal and temperate lakes (72, 73). The lake surface area corresponding to the two depth interval regions of the littoral zone (0 to 4 m and 4 to 10 m) was derived from morphometric relations based on maximum depth (74) that was itself derived from the mean depth reported in HydroLAKES (29) using a ratio of average depth over maximum depth of 0.464 (75).

## Statistical analysis

Linear regressions were tested at 0.05 level ( $r^2$  and  $P$ ) using GraphPad Prism (version 7).

## SUPPLEMENTARY MATERIALS

Supplementary material for this article is available at <https://science.org/doi/10.1126/sciadv.abi8716>

## REFERENCES AND NOTES

1. J. J. Cole, N. F. Caraco, G. W. Kling, T. K. Kratz, Carbon dioxide supersaturation in the surface waters of lakes. *Science* **265**, 1568–1570 (1994).
2. S. Sobek, L. J. Tranvik, J. J. Cole, Temperature independence of carbon dioxide supersaturation in global lakes. *Global Biogeochem. Cycles* **19**, GB2003 (2005).
3. D. Bastviken, L. J. Tranvik, J. A. Downing, P. M. Crill, A. Enrich-Prast, Freshwater methane emissions offset the continental carbon sink. *Science* **331**, 50–50 (2011).
4. P. A. Raymond, J. Hartmann, R. Lauerwald, S. Sobek, C. McDonald, M. Hoover, D. Butman, R. Striegl, E. Mayorga, C. Humborg, P. Kortelainen, H. Dürr, M. Meybeck, P. Ciais, P. Guth, Global carbon dioxide emissions from inland waters. *Nature* **503**, 355–359 (2013).

5. T. DelSontro, J. J. Beaulieu, J. A. Downing, Greenhouse gas emissions from lakes and impoundments: Upscaling in the face of global change. *Limnol. Oceanogr. Lett.* **3**, 64–75 (2018).
6. W. M. Lewis Jr., Tropical limnology. *Annu. Rev. Ecol. Syst.* **18**, 159–184 (1987).
7. J. Langeveld, A. F. Bouwman, W. J. van Hoek, L. Vilmin, A. H. W. Beusen, J. M. Mogollón, J. J. Middelburg, Estimating dissolved carbon concentrations in global soils: A global database and model. *SN Appl. Sci.* **2**, 1626 (2020).
8. J. F. Lapierre, P. A. del Giorgio, Geographical and environmental drivers of regional differences in the lake pCO<sub>2</sub> versus DOC relationship across northern landscapes. *J. Geophys. Res.* **117**, G03015 (2012).
9. H. Marotta, C. M. Duarte, S. Sobek, A. Enrich-Prast, Large CO<sub>2</sub> disequilibria in tropical lakes. *Global Biogeochem. Cycles* **23**, GB4022 (2009).
10. S. Kosten, F. Roland, D. M. L. Da Motta Marques, E. H. Van Nes, N. Mazzeo, L. da S. L. Sternberg, M. Scheffer, J. J. Cole, Climate-dependent CO<sub>2</sub> emissions from lakes. *Global Biogeochem. Cycles* **24**, GB2007 (2010).
11. J. R. Helms, A. Stubbins, J. D. Ritchie, E. C. Minor, D. J. Kieber, K. Mopper, Absorption spectral slopes and slope ratios as indicators of molecular weight, source, and photobleaching of chromophoric dissolved organic matter. *Limnol. Oceanogr.* **53**, 955–969 (2008).
12. P. A. del Giorgio, R. H. Peters, Patterns in planktonic P:R ratios in lakes: Influence of lake trophy and dissolved organic carbon. *Limnol. Oceanogr.* **39**, 772–787 (1994).
13. S. Sobek, G. Algesten, A.-K. Bergström, M. Jansson, L. Tranvik, The catchment and climate regulation of pCO<sub>2</sub> in boreal lakes. *Glob. Change Biol.* **9**, 630–641 (2003).
14. J. P. Casas-Ruiz, J. Jakobsson, P. A. del Giorgio, The role of lake morphology in modulating surface water carbon concentrations in boreal lakes. *Environ. Res. Lett.* **16**, 074037 (2021).
15. K. Sand-Jensen, P. A. Staehr, Scaling of pelagic metabolism to size, trophy and forest cover in small Danish lakes. *Ecosystems* **10**, 128–142 (2007).
16. R. Wanninkhof, Relationship between wind speed and gas exchange over the ocean. *J. Geophys. Res.* **97**, 7373–7382 (1992).
17. A. V. Borges, F. Darchambeau, T. Lambert, C. Morana, G. H. Allen, E. Tambwe, A. Toengaho Sembaito, T. Mambo, J. Nlandu Wabakhangazi, J.-P. Descy, C. R. Teodoru, S. Bouillon, Variations in dissolved greenhouse gases (CO<sub>2</sub>, CH<sub>4</sub>, N<sub>2</sub>O) in the Congo River network overwhelmingly driven by fluvial-wetland connectivity. *Biogeosciences* **16**, 3801–3834 (2019).
18. C. S. Reynolds, *The Ecology of Phytoplankton* (Cambridge Univ. Press, 2006).
19. M. J. Bogard, P. A. del Giorgio, L. Boutet, M. C. G. Chaves, Y. T. Prairie, A. Merante, A. M. Derry, Oxidic water column methanogenesis as a major component of aquatic CH<sub>4</sub> fluxes. *Nat. Commun.* **5**, 5350 (2014).
20. M. Bižić, T. Klintzsch, D. Ionescu, M. Y. Hindiyeh, M. Günthel, A. M. Muro-Pastor, W. Eckert, T. Ulrich, F. Keppler, H.-P. Grossart, Aquatic and terrestrial cyanobacteria produce methane. *Sci. Adv.* **6**, eaax5343 (2020).
21. H.-P. Grossart, K. Frindte, C. Dziallas, W. Eckert, K. W. Tang, Microbial methane production in oxygenated water column of an oligotrophic lake. *Proc. Natl. Acad. Sci. U.S.A.* **108**, 19657–19661 (2011).
22. C. Morana, S. Bouillon, V. Nolla-Ardévol, F. A. E. Roland, W. Okello, J.-P. Descy, A. Nankabirwa, E. Nabafu, D. Springael, A. V. Borges, Methane paradox in tropical lakes? Sedimentary fluxes rather than pelagic production in oxic conditions sustain methanotrophy and emissions to the atmosphere. *Biogeosciences* **17**, 5209–5221 (2020).
23. R. I. Jones, The influence of humic substances on lacustrine planktonic food chains. *Hydrobiologia* **229**, 73–91 (1992).
24. G. Yvon-Durocher, A. P. Allen, D. Bastviken, R. Conrad, C. Gudas, A. St-Pierre, N. Thanh-Duc, P. A. del Giorgio, Methane fluxes show consistent temperature dependence across microbial to ecosystem scales. *Nature* **507**, 488–491 (2014).
25. P. Kankaala, J. Huotari, T. Tulonen, A. Ojala, Lake-size dependent physical forcing drives carbon dioxide and methane effluxes from lakes in a boreal landscape. *Limnol. Oceanogr.* **58**, 1915–1930 (2013).
26. M. A. Holgerson, P. A. Raymond, Large contribution to inland water CO<sub>2</sub> and CH<sub>4</sub> emissions from very small ponds. *Nat. Geosci.* **9**, 222–226 (2016).
27. S. R. Alin, T. C. Johnson, Carbon cycling in large lakes of the world: A synthesis of production, burial, and lake-atmosphere exchange estimates. *Global Biogeochem. Cycles* **21**, GB3002 (2007).
28. G. Abril, S. Bouillon, F. Darchambeau, C. R. Teodoru, T. R. Marwick, F. Tamooh, F. O. Omengo, N. Geeraert, L. Deirmendjian, P. Polesnaere, A. V. Borges, Technical note: Large overestimation of pCO<sub>2</sub> calculated from pH and alkalinity in acidic, organic-rich freshwaters. *Biogeosciences* **12**, 67–78 (2015).
29. M. L. Messenger, B. Lehner, G. Grill, I. Nedeva, O. Schmitt, Estimating the volume and age of water stored in global lakes using a geo-statistical approach. *Nat. Commun.* **7**, 13603 (2016).
30. B. Pham-Duc, F. Sylvestre, F. Papa, F. Frappart, C. Bouchez, J.-F. Crétau, The Lake Chad hydrology under current climate change. *Sci. Rep.* **10**, 5498 (2020).
31. R. Lauerwald, P. Regnier, V. Figueiredo, A. Enrich-Prast, D. Bastviken, B. Lehner, T. Maavara, P. Raymond, Natural lakes are a minor global source of N<sub>2</sub>O to the atmosphere. *Global Biogeochem. Cycles* **33**, 1564–1581 (2019).
32. J. M. Melack, L. L. Hess, M. Gastil, B. R. Forsberg, S. K. Hamilton, I. B. T. Lima, E. M. L. M. Novo, Regionalization of methane emissions in the Amazon Basin with microwave remote sensing. *Glob. Change Biol.* **10**, 530–544 (2004).
33. M. Saunois, P. Bousquet, B. Poulter, A. Peregon, P. Ciais, J. G. Canadell, E. J. Dlugokencky, G. Etiope, D. Bastviken, S. Houweling, G. Janssens-Maenhout, F. N. Tubiello, S. Castaldi, R. B. Jackson, M. Alexe, V. K. Arora, D. J. Beerling, P. Bergamaschi, D. R. Blake, G. Brailsford, V. Brovkin, L. Bruhwiler, C. Crevoisier, P. Crill, K. Covey, C. Curry, C. Frankenberg, N. Gedney, L. Höglund-Isaksson, M. Ishizawa, A. Ito, F. Joos, H.-S. Kim, T. Kleinen, P. Krummel, J.-F. Lamarque, R. Langenfelds, R. Locatelli, T. Machida, S. Maksyutov, K. C. McDonald, J. Marshall, J. R. Melton, I. Morino, V. Naik, S. O'Doherty, F.-J. W. Parmentier, P. K. Patra, C. Peng, S. Peng, G. P. Peters, I. Pison, C. Prigent, R. Prinn, M. Ramonet, W. J. Riley, M. Saito, M. Santini, R. Schroeder, I. J. Simpson, R. Spahni, P. Steele, A. Takizawa, B. F. Thornton, H. Tian, Y. Tohjima, N. Viovy, A. Voulgarakis, M. van Weele, G. R. van der Werf, R. Weiss, C. Wiedinmyer, D. J. Wilton, A. Wiltshire, D. Worthy, D. Wunch, X. Xu, Y. Yoshida, B. Zhang, Z. Zhang, Q. Zhu, The global methane budget. *Earth Syst. Sci. Data* **8**, 697–751 (2016).
34. A. V. Borges, F. Darchambeau, C. R. Teodoru, T. R. Marwick, F. Tamooh, N. Geeraert, F. O. Omengo, F. Guérin, T. Lambert, C. Morana, E. Okuku, S. Bouillon, Globally significant greenhouse gas emissions from African inland waters. *Nat. Geosci.* **8**, 637–642 (2015).
35. A. V. Borges, G. Abril, F. Darchambeau, C. R. Teodoru, J. Deborde, L. O. Vidal, T. Lambert, S. Bouillon, Divergent biophysical controls of aquatic CO<sub>2</sub> and CH<sub>4</sub> in the World's two largest rivers. *Sci. Rep.* **5**, 15614 (2015).
36. J. F. Talling, The annual cycle of stratification and phytoplankton growth in Lake Victoria (East Africa). *Int. Rev. gesamten Hydrobiol., Syst. Beih.* **51**, 545–621 (1966).
37. L. Pinho, C. M. Duarte, H. Marotta, A. Enrich-Prast, Temperature dependence of the relationship between pCO<sub>2</sub> and dissolved organic carbon in lakes. *Biogeosciences* **13**, 865–871 (2016).
38. K. Toming, J. Kotta, E. Uuemaa, S. Sobek, T. Kutser, L. J. Tranvik, Predicting lake dissolved organic carbon at a global scale. *Sci. Rep.* **10**, 8471 (2020).
39. C. Verpoorter, T. Kutser, D. A. Seekell, L. J. Tranvik, A global inventory of lakes based on high-resolution satellite imagery. *Geophys. Res. Lett.* **41**, 6396–6402 (2014).
40. T. W. Drake, P. A. Raymond, R. G. M. Spencer, Terrestrial carbon inputs to inland waters: A current synthesis of estimates and uncertainty. *Limnol. Oceanogr. Lett.* **3**, 132–142 (2018).
41. J. J. Cole, Y. T. Prairie, N. F. Caraco, W. H. McDowell, L. J. Tranvik, R. G. Striegl, C. M. Duarte, P. Kortelainen, J. A. Downing, J. J. Middelburg, J. Melack, Plumbing the global carbon cycle: Integrating inland waters into the terrestrial carbon budget. *Ecosystems* **10**, 172–185 (2007).
42. R. Kindler, J. Siemens, K. Kaiser, D. C. Walmsley, C. Bernhofer, N. Buchmann, P. Cellier, W. Eugster, G. Gleixner, T. Grunwald, A. Heim, A. Ibrom, S. K. Jones, M. Jones, K. Klumpp, W. Kutsch, L. K. Steenberg, S. Lehuger, B. Loubet, R. McKenzie, E. Moors, B. Osborne, K. Pilegaard, C. Rebmann, M. Saunders, M. W. I. Schmidt, M. Schrumppf, J. Seyferth, U. Skiba, J.-F. Soussana, M. A. Sutton, C. Tefs, B. Vowinkel, M. J. Zeeman, M. Kaupenjohann, Dissolved carbon leaching from soil is a crucial component of net ecosystem carbon balance. *Glob. Change Biol.* **17**, 1167–1185 (2011).
43. W. Liang, W. Zhang, Z. Jin, J. Yan, Y. Lü, S. Wang, B. Fu, S. Li, Q. Ji, F. Gou, S. Fu, S. An, F. Wang, Estimation of global grassland net ecosystem carbon exchange using a model tree ensemble approach. *J. Geophys. Res. Biogeosci.* **125**, e2019JG005034 (2020).
44. J. Zeng, T. Matsunaga, Z.-H. Tan, N. Saigusa, T. Shirai, Y. Tang, S. Peng, Y. Fukuda, Global terrestrial carbon fluxes of 1999–2019 estimated by upscaling eddy covariance data with a random forest. *Sci. Data* **7**, 313 (2020).
45. W. Ludwig, J. L. Probst, S. Kempe, Predicting the oceanic input of organic carbon by continental erosion. *Global Biogeochem. Cycles* **10**, 23–41 (1996).
46. G. Abril, A. V. Borges, Ideas and perspectives: Carbon leaks from flooded land: Do we need to replumb the inland water active pipe? *Biogeosciences* **16**, 769–784 (2019).
47. A. K. Aufdenkampe, E. Mayorga, P. A. Raymond, J. M. Melack, S. C. Doney, S. R. Alin, R. E. Aalto, K. Yoo, Riverine coupling of biogeochemical cycles between land, oceans, and atmosphere. *Front. Ecol. Environ.* **9**, 53–60 (2011).
48. M. J. Ngochera, H. A. Bootsma, Spatial and temporal dynamics of pCO<sub>2</sub> and CO<sub>2</sub> flux in tropical Lake Malawi. *Limnol. Oceanogr.* **65**, 1594–1607 (2020).
49. A. V. Borges, G. Abril, B. Delille, J.-P. Descy, F. Darchambeau, Diffusive methane emissions to the atmosphere from Lake Kivu (Eastern Africa). *J. Geophys. Res.* **116**, G03032 (2011).
50. P. Kortelainen, T. Larmola, M. Rantakari, S. Juutinen, J. Alm, P. J. Martikainen, Lakes as nitrous oxide sources in the boreal landscape. *Glob. Change Biol.* **26**, 1432–1445 (2020).
51. E. O. Okuku, S. Bouillon, M. Tole, A. V. Borges, Diffusive emissions of methane and nitrous oxide from a cascade of tropical hydropower reservoirs in Kenya. *Lakes Reserv.* **24**, 127–135 (2019).

52. C. R. Teodoru, F. C. Nyoni, A. V. Borges, F. Darchambeau, I. Nyambe, S. Bouillon, Spatial variability and temporal dynamics of greenhouse gas (CO<sub>2</sub>, CH<sub>4</sub>, N<sub>2</sub>O) concentrations and fluxes along the Zambezi River mainstem and major tributaries. *Biogeosciences* **12**, 2431–2453 (2015).
53. G. Abril, F. Guérin, S. Richard, R. Delmas, C. Galy-Lacaux, P. Gosse, A. Tremblay, L. Varfalvy, M. Aurelio Dos Santos, B. Matvienko, Carbon dioxide and methane emissions and the carbon budget of a 10-year old tropical reservoir (Petit Saut, French Guiana). *Global Biogeochem. Cycles* **19**, GB4007 (2005).
54. L. Deirmendjian, J.-P. Descy, C. Morana, W. Okello, M. P. Stoyneva-Gärtner, S. Bouillon, A. V. Borges, Limnological changes in Lake Victoria since the mid-20<sup>th</sup> century. *Freshw. Biol.* **66**, 1630–1647 (2021).
55. A. V. Borges, C. Morana, S. Bouillon, P. Servais, J.-P. Descy, F. Darchambeau, Carbon cycling of Lake Kivu (East Africa): Net autotrophy in the epilimnion and emission of CO<sub>2</sub> to the atmosphere sustained by geogenic inputs. *PLoS ONE* **9**, e109500 (2014).
56. S. Yamamoto, J. B. Alcauskas, T. E. Crozier, Solubility of methane in distilled water and seawater. *J. Chem. Eng. Data* **21**, 78–80 (1976).
57. R. F. Weiss, B. A. Price, Nitrous oxide solubility in water and seawater. *Mar. Chem.* **8**, 347–359 (1980).
58. C. W. Hunt, L. Snyder, J. E. Salisbury, D. Vandemark, W. H. McDowell, SIPC02: A simple, inexpensive surface water pCO<sub>2</sub> sensor. *Limnol. Oceanogr. Methods* **15**, 291–301 (2017).
59. M. D. Mackey, D. J. Mackey, H. W. Higgins, S. W. Wright, CHEMTAX—A program for estimating class abundances from chemical markers: Application to HPLC measurements of phytoplankton. *Mar. Ecol. Progr. Ser.* **144**, 265–283 (1996).
60. APHA, *Standard Methods For The Examination Of Water And Wastewater* (American Public Health Association, 1998).
61. Standing Committee Of Analysts, *Ammonia in Waters: Methods for the Examination of Waters and Associated Materials* (H.M.S.O., 1981), 16 pp.
62. E. Fluet-Chouinard, B. Lehner, L.-M. Rebelo, F. Papa, S. K. Hamilton, Development of a global inundation map at high spatial resolution from topographic downscaling of coarse-scale remote sensing data. *Remote Sens Environ.* **158**, 348–361 (2015).
63. S. E. Fick, R. J. Hijmans, WorldClim 2: New 1km spatial resolution climate surfaces for global land areas. *Int. J. Climatol.* **37**, 4302–4315 (2017).
64. J. J. Cole, N. F. Caraco, Atmospheric exchange of carbon dioxide in a low-wind oligotrophic lake measured by the addition of SF<sub>6</sub>. *Limnol. Oceanogr.* **43**, 647–656 (1998).
65. B. Lehner, K. Verdin, A. Jarvis, New global hydrography derived from spaceborne elevation data. *Eos* **89**, 93–94 (2008).
66. J.-F. Lapiere, D. A. Seekell, C. T. Filstrup, S. M. Collins, C. Emi Fergus, P. A. Soranno, K. S. Cheruvellil, Continental-scale variation in controls of summer CO<sub>2</sub> in United States lakes. *J. Geophys. Res. Biogeosci.* **122**, 875–885 (2017).
67. S. C. Maberly, R. A. O'Donnell, R. I. Woolway, M. E. J. Cutler, M. Gong, I. D. Jones, C. J. Merchant, C. A. Miller, E. Politi, E. M. Scott, S. J. Thackeray, A. N. Tyler, Global lake thermal regions shift under climate change. *Nat. Commun.* **11**, 1232 (2020).
68. J. Verbeke, Recherches écologiques sur la faune des grands lacs de l'est du Congo belge. Bulletin de l'Institut royal des Sciences naturelles de Belgique : Résultats scientifiques de l'exploration hydrobiologique (1952-1954) des lacs Kivu, Edouard et Albert (1957).
69. S. E. Hamilton, "Creation of a bathymetric map of Lake Victoria, Africa" (2016); <http://dx.doi.org/10.7910/DVN/SOEKNR>.
70. S. MacIntyre, A. T. Crowe, A. Cortés, L. Arneborg, Turbulence in a small arctic pond. *Limnol. Oceanogr.* **63**, 2337–2358 (2018).
71. D. Vachon, Y. T. Prairie, The ecosystem size and shape dependence of gas transfer velocity versus wind speed relationships in lakes. *Can. J. Fish. Aquat. Sci.* **70**, 1757–1764 (2013).
72. T. DelSontro, L. Boutet, A. St-Pierre, P. A. del Giorgio, Y. T. Prairie, Methane ebullition and diffusion from northern ponds and lakes regulated by the interaction between temperature and system productivity. *Limnol. Oceanogr.* **61**, S62–S77 (2016).
73. M. Wik, P. M. Crill, R. K. Varner, D. Bastviken, Multiyear measurements of ebullitive methane flux from three subarctic lakes. *J. Geophys. Res. Biogeosci.* **118**, 1307–1321 (2013).
74. J. Håkan, A. A. Brolin, L. Håkanson, New approaches to the modelling of lake basin morphometry. *Environ. Model. Assess.* **12**, 213–228 (2007).
75. R. G. Wetzel, *Limnology: Lake & River Ecosystems* (Academic Press, ed. 3, 2001), p. 429.
76. P. A. del Giorgio, J. J. Cole, N. F. Caraco, R. H. Peters, Linking planktonic biomass and metabolism to net gas fluxes in northern temperate lakes. *Ecology* **80**, 1422–1431 (1999).
77. K. Finlay, P. R. Leavitt, A. Patoine, B. Wissel, Magnitudes and controls of organic and inorganic carbon flux through a chain of hardwater lakes on the northern Great Plains. *Limnol. Oceanogr.* **55**, 1551–1564 (2010).
78. H. Marotta, C. M. Duarte, L. Pinho, A. Enrich-Prast, Rainfall leads to increased pCO<sub>2</sub> in Brazilian coastal lakes. *Biogeosciences* **7**, 1607–1614 (2010).
79. M. A. Xenopoulos, D. M. Lodge, J. Frenness, T. A. Kreps, S. D. Bridgman, E. Grossman, C. J. Jackson, Regional comparisons of watershed determinants of dissolved organic carbon in temperate lakes from the Upper Great Lakes region and selected regions globally. *Limnol. Oceanogr.* **48**, 2321–2334 (2003).
80. J. A. Zwart, Z. J. Hanson, J. Vanderwall, D. Bolster, A. Hamlet, S. E. Jones, Spatially explicit, regional-scale simulation of lake carbon fluxes. *Global Biogeochem. Cycles* **32**, 1276–1293 (2018).
81. P. A. Staehr, L. Baastrup-Spohr, K. Sand-Jensen, C. Stedmon, Lake metabolism scales with lake morphometry and catchment conditions. *Aquat. Sci.* **74**, 155–169 (2012).
82. J. P. Casas-Ruiz, R. H. S. Hutchins, P. A. del Giorgio, Total aquatic carbon emissions across the boreal biome of Québec driven by watershed slope. *J. Geophys. Res. Biogeosci.* **126**, e2020JG005863 (2021).
83. G. W. Kling, Comparative transparency, depth of mixing, and stability of stratification in lakes of Cameroon, West Africa. *Limnol. Oceanogr.* **33**, 27–40 (1988).
84. E. G. Stets, D. Butman, C. P. McDonald, S. M. Stackpole, M. D. DeGrandpre, R. G. Striegl, Carbonate buffering and metabolic controls on carbon dioxide in rivers. *Global Biogeochem. Cycles* **31**, 663–677 (2017).
85. J. Schenk, H. O. Sawakuchi, A. K. Siczko, G. Pajala, D. Rudberg, E. Hagberg, K. Fors, H. Laudon, J. Karlsson, D. Bastviken, Methane in lakes: Variability in stable carbon isotopic composition and the potential importance of groundwater input. *Front. Earth Sci.* **9**, 722215 (2021).
86. W. E. West, K. P. Creamer, S. E. Jones, Productivity and depth regulate lake contributions to atmospheric methane. *Limnol. Oceanogr.* **61**, S51–S61 (2016).
87. D. Bastviken, J. Cole, M. Pace, L. Tranvik, Methane emissions from lakes: Dependence of lake characteristics, two regional assessments, and a global estimate. *Global Biogeochem. Cycles* **18**, GB4009 (2004).
88. F. A. E. Roland, F. Darchambeau, C. Morana, A. V. Borges, Nitrous oxide and methane seasonal variability in the epilimnion of a large tropical meromictic lake (Lake Kivu, East-Africa). *Aquat. Sci.* **79**, 209–218 (2017).
89. K. Desrosiers, T. DelSontro, P. A. del Giorgio, Disproportionate contribution of vegetated habitats to the CH<sub>4</sub> and CO<sub>2</sub> budgets of a boreal lake. *Ecosystems*, (2021).
90. E. S. Oliveira Junior, T. J. H. M. van Bergen, J. Nauta, A. Budiša, R. C. H. Aben, S. T. J. Weideveld, C. A. de Souza, C. C. Muniz, J. Roelofs, L. P. M. Lamers, S. Kosten, Water hyacinth's effect on greenhouse gas fluxes: A field study in a wide variety of tropical water bodies. *Ecosystems* **24**, 988–1004 (2021).
91. J. E. Fernández, F. Peeters, H. Hofmann, On the methane paradox: Transport from shallow water zones rather than in situ methanogenesis is the major source of CH<sub>4</sub> in the open surface water of lakes. *J. Geophys. Res. Biogeosci.* **121**, 2717–2726 (2016).
92. T. DelSontro, P. A. del Giorgio, Y. T. Prairie, No longer a paradox: The interaction between physical transport and biological processes explains the spatial distribution of surface water methane within and across lakes. *Ecosystems* **21**, 1073–1087 (2018).
93. H. Wang, L. Yang, W. Wang, J. Lu, C. Yin, Nitrous oxide (N<sub>2</sub>O) fluxes and their relationships with water-sediment characteristics in a hyper-eutrophic shallow lake, China. *J. Geophys. Res.* **112**, G01005 (2007).
94. C. Soued, P. A. del Giorgio, R. Maranger, Nitrous oxide sinks and emissions in boreal aquatic networks in Quebec. *Nat. Geosci.* **9**, 116–120 (2015).
95. M. Mengis, R. Gächter, B. Wehrli, Sources and sinks of nitrous oxide (N<sub>2</sub>O) in deep lakes. *Biogeochemistry* **38**, 281–301 (1997).
96. K. Finlay, P. R. Leavitt, B. Wissel, Y. T. Prairie, Regulation of spatial and temporal variability of carbon flux in six hard-water lakes of the northern Great Plains. *Limnol. Oceanogr.* **54**, 2553–2564 (2009).
97. A. Baccini, N. Laporte, S. J. Goetz, M. Sun, H. Dong, A first map of tropical Africa's above-ground biomass derived from satellite imagery. *Environ. Res. Lett.* **3**, 045011 (2008).
98. P. Mayaux, E. Bartholomé, S. Fritz, A. Belward, A new land-cover map of Africa for the year 2000. *J. Biogeogr.* **31**, 861–877 (2004).
99. D. Bastviken, A. L. Santoro, H. Marotta, L. Q. Pinho, D. F. Calheiros, P. Crill, A. Enrich-Prast, Methane emissions from Pantanal, South America, during the low water season: Toward more comprehensive sampling. *Environ. Sci. Technol.* **44**, 5450–5455 (2010).
100. P. M. Barbosa, J. M. Melack, J. H. F. Amaral, S. MacIntyre, D. Kasper, A. Cortés, V. F. Farjalla, B. R. Forsberg, Dissolved methane concentrations and fluxes to the atmosphere from a tropical floodplain lake. *Biogeochemistry* **148**, 129–151 (2020).
101. P. M. Crill, K. B. Bartlett, J. O. Wilson, D. I. Sebacher, R. C. Harriss, J. M. Melack, S. MacIntyre, L. Lesack, L. Smith-Morrill, Tropospheric methane from an Amazonian floodplain lake. *J. Geophys. Res.* **93**, 1564–1570 (1988).
102. D. Engle, J. M. Melack, Methane emissions from an Amazon floodplain lake: Enhanced release during episodic mixing and during falling water. *Biogeochemistry* **51**, 71–90 (2000).
103. A. H. Devol, J. E. Richey, W. A. Clark, S. L. King, L. A. Martinelli, Methane emissions to the troposphere from the Amazon Floodplain. *J. Geophys. Res.* **93**, 1583–1592 (1988).
104. L. K. Smith, W. M. Lewis, J. P. Chanton, G. Cronin, S. K. Hamilton, Methane emissions from the Orinoco River floodplain, Venezuela. *Biogeochemistry* **51**, 113–140 (2000).



105. K. Attemeyer, S. Flury, R. Jayakumar, P. Fiener, K. Steger, V. Arya, F. Wilken, R. van Geldern, K. Premke, Invasive floating macrophytes reduce greenhouse gas emissions from a small tropical lake. *Sci. Rep.* **6**, 20424 (2016).
106. P. M. Barbosa, V. F. Farjalla, J. M. Melack, J. H. F. Amaral, J. S. da Silva, B. R. Forsberg, High rates of methane oxidation in an Amazon floodplain lake. *Biogeochemistry* **137**, 351–365 (2018).
107. R. E. Hecky, R. Mugidde, P. S. Ramlal, M. R. Talbot, G. W. Kling, Multiple stressors cause rapid ecosystem change in Lake Victoria. *Freshw. Biol.* **55**, 19–42 (2010).
108. P. M. Barbosa, J. M. Melack, V. F. Farjalla, J. H. F. Amaral, V. Scofield, B. R. Forsberg, Diffusive methane fluxes from Negro, Solimões and Madeira rivers and fringing lakes in the Amazon basin. *Limnol. Oceanogr.* **61**, S221–S237 (2016).
109. G. Abril, J.-M. Martinez, L. F. Artigas, P. Moreira-Turcq, M. F. Benedetti, L. Vidal, T. Meziane, J.-H. Kim, M. C. Bernardes, N. Savoye, J. Deborde, P. Albéric, M. F. L. Souza, E. L. Souza, F. Roland, Amazon river carbon dioxide outgassing fuelled by wetlands. *Nature* **505**, 395–398 (2014).
110. B. Panneer Selvam, S. Natchimuthu, L. Arunachalam, D. Bastviken, Methane and carbon dioxide emissions from inland waters in India - implications for large scale greenhouse gas balances. *Glob. Change Biol.* **20**, 3397–3407 (2014).
111. M. U. Mendoza-Pascual, M. Itoh, J. I. Aguilar, K. S. A. R. Padilla, R. D. S. Papa, N. Okuda, Controlling factors of methane dynamics in tropical lakes of different depths. *J. Geophys. Res. Biogeosci.* **126**, e2020JG005828 (2021).
112. D. Tonetta, P. A. Staehr, B. Obrador, L. P. Mello Brandão, L. Silva Brighenti, M. Mello Petrucio, F. A. Rodrigues Barbosa, J. F. Bezerra-Neto, Effects of nutrients and organic matter inputs in the gases CO<sub>2</sub> and O<sub>2</sub>: A mesocosm study in a tropical lake. *Limnologia* **69**, 1–9 (2018).
113. P. A. Macklin, I. G. N. A. Suryaputra, D. T. Maher, I. R. Santos, Carbon dioxide dynamics in a lake and a reservoir on a tropical island (Bali, Indonesia). *PLOS ONE* **13**, e0198678 (2018).
114. P. Albéric, M. A. P. Pérez, P. Moreira-Turcq, M. F. Benedetti, S. Bouillon, G. Abril, Variation of the isotopic composition of dissolved organic carbon during the runoff cycle in the Amazon River and the floodplains. *C. R. Geosci.* **350**, 65–75 (2018).
115. J. H. F. Amaral, J. M. Melack, P. M. Barbosa, S. MacIntyre, D. Kasper, A. Cortés, T. S. Freire Silva, R. Nunes de Sousa, B. R. Forsberg, Carbon dioxide fluxes to the atmosphere from waters within flooded forests in the Amazon basin. *J. Geophys. Res. Biogeosci.* **125**, e2019JG005293 (2020).
116. M. Call, C. J. Sanders, A. Enrich-Prast, L. Sanders, H. Marotta, I. R. Santos, D. T. Maher, Radon-traced pore-water as a potential source of CO<sub>2</sub> and CH<sub>4</sub> to receding black and clear water environments in the Amazon Basin. *Limnol. Oceanogr. Lett.* **3**, 375–383 (2018).
117. S. Sobek, L. J. Tranvik, Y. P. Prairie, P. Kortelainen, J. J. Cole, Patterns and regulation of dissolved organic carbon: An analysis of 7,500 widely distributed lakes. *Limnol. Oceanogr.* **52**, 1208–1219 (2007).
118. M. Frankignoulle, A. Borges, R. Biondo, A new design of equilibrator to monitor carbon dioxide in highly dynamic and turbid environments. *Water Res.* **35**, 1344–1347 (2001).
119. G. W. Kling, M. A. Clark, G. N. Wagner, H. R. Compton, A. M. Humphrey, J. D. Devine, W. C. Evans, J. P. Lockwood, M. L. Tuttle, E. J. Koenigsberg, The 1986 Lake Nyos gas disaster in Cameroon, West Africa. *Science* **236**, 169–175 (1987).

**Acknowledgments:** We are grateful to crews of *RV Hammerkop* and the *Maman Benita* for support during the sampling expeditions in Lakes Victoria and Tanganyika; to C. M. Balagizi for help during the sampling of the Masisi lakes; to the team from the Institut Supérieur Pédagogique Bukavu for help during the sampling in Lake Kivu; to the Katwe marine police officers, A. Nankabirwa and E. Nabafu for help during sampling in Lakes Edward and George; to M.-V. Commarieu, B. Leporcq, Z. Kelemen, and T. Bousmanne for analytical support; to TCarta for the GIS of Lake Tanganyika bathymetry; and to four anonymous reviewers for comments on the initial submission. L.D., C.M., and F.A.E.R. are postdoctoral researchers at the FNRS, and A.V.B. is a Research Director at the FNRS. **Funding:** This work was supported by Belgian Federal Science Policy Office grant SD/AR/02A, Belgian Federal Science Policy Office grant BR/154/A1/HIPE, Fonds National de la Recherche Scientifique grant 2.4.598.07, Fonds National de la Recherche Scientifique grant 2.4.515.11, Fonds National de la Recherche Scientifique grant T.0246.13, Fonds National de la Recherche Scientifique grant J.0009.15, Fonds National de la Recherche Scientifique grant U.N024.17, Fonds National de la Recherche Scientifique grant T.0156.18, Fonds National de la Recherche Scientifique grant J.0013.19, Fonds National de la Recherche Scientifique grant T.0027.20, Fonds National de la Recherche Scientifique grant J.0015.21, EU Marie Skłodowska Curie Fellowship grant H2020-MSCA-IF-2017 no. 796707, KU Leuven Special Research Fund, Fonds Wetenschappelijk Onderzoek, Fonds Agathon de Potter, and Fonds Léopold III pour l'Exploration et la Conservation de la Nature. **Author contributions:** Conceptualization: A.V.B. Sample collection: A.V.B., L.D., S.B., W.O., T.L., F.A.E.R., V.F.R., N.R.G.V., F.D., I.A.K., and C.M. Sample analysis: A.V.B., L.D., S.B., T.L., F.A.E.R., V.F.R., N.R.G.V., F.D., J.-P.D., and C.M. GIS data extraction and analysis: A.V.B., L.D., T.L., G.H.A., and C.M. Writing (original draft): A.V.B. Writing (review and editing): L.D., S.B., W.O., T.L., F.A.E.R., V.F.R., N.R.G.V., F.D., I.A.K., J.-P.D., G.H.A., and C.M. **Competing interests:** The authors declare that they have no competing interests. **Data and materials availability:** The CO<sub>2</sub>, CH<sub>4</sub>, and N<sub>2</sub>O data can be downloaded from <https://doi.org/10.5281/zenodo.6025626>. All data needed to evaluate the conclusions in the paper are present in the paper and/or the Supplementary Materials.

Submitted 6 April 2021

Accepted 9 May 2022

Published 24 June 2022

10.1126/sciadv.abi8716